

A SYMMETRIZED PARAMETRIC FINITE ELEMENT METHOD FOR ANISOTROPIC SURFACE DIFFUSION IN 3D

WEIZHU BAO* AND YIFEI LI†

Abstract. For the evolution of a closed surface under anisotropic surface diffusion with a general anisotropic surface energy $\gamma(\mathbf{n})$ in three dimensions (3D), where \mathbf{n} is the unit outward normal vector, by introducing a novel symmetric positive definite surface energy matrix $\mathbf{Z}_k(\mathbf{n})$ depending on a stabilizing function $k(\mathbf{n})$ and the Cahn-Hoffman $\boldsymbol{\xi}$ -vector, we present a new symmetrized variational formulation for anisotropic surface diffusion with weakly or strongly anisotropic surface energy, which preserves two important structures including volume conservation and energy dissipation. Then we propose a structural-preserving parametric finite element method (SP-PFEM) to discretize the symmetrized variational problem, which preserves the volume in the discretized level. Under a relatively mild and simple condition on $\gamma(\mathbf{n})$, we show that SP-PFEM is unconditionally energy-stable for almost all anisotropic surface energies $\gamma(\mathbf{n})$ arising in practical applications. Extensive numerical results are reported to demonstrate the efficiency and accuracy as well as energy dissipation of the proposed SP-PFEM for solving anisotropic surface diffusion in 3D.

Key words. Anisotropic surface diffusion, Cahn-Hoffman $\boldsymbol{\xi}$ -vector, anisotropic surface energy, parametric finite element method, structure-preserving, energy-stable, surface energy matrix

AMS subject classifications. 65M60, 65M12, 35K55, 53C44

1. Introduction. In materials science and solid-state physics as well as many other applications, surface energy is usually anisotropic due to lattice orientational anisotropy at material interfaces and/or surfaces [39, 24]. The anisotropic surface energy generates **anisotropic surface diffusion** – an important and general process involving the motion of adatoms, molecules and atomic clusters (adparticles) – at materials surfaces and interfaces in solids [18]. The anisotropic surface diffusion is an important kinetics and/or mechanism in surface phase formation [16, 19], epitaxial growth [23, 25], heterogeneous catalysis [26], and other areas in materials/surface science [40]. It has significant and manifested applications in solid-state physics and materials science as well as computational geometry, such as solid-state dewetting [29, 35, 41, 40, 45], crystal growth of nanomaterials [14], evolution of voids in microelectronic circuits [33, 43], morphology development of alloys [2], quantum dots manufacturing [1], deformation of images [20], etc.

As is shown in Figure 1.1, for a closed surface $S := S(t)$ in three dimensions (3D) associated with a given anisotropic surface energy $\gamma(\mathbf{n})$, where $t \geq 0$ is time and $\mathbf{n} = (n_1, n_2, n_3)^T \in \mathbb{S}^2$ represents the outward unit normal vector satisfying $|\mathbf{n}| := \sqrt{n_1^2 + n_2^2 + n_3^2} = 1$, the motion by anisotropic surface diffusion of the surface is described by the following geometric flow [34, 29, 35, 41, 40, 45]:

$$(1.1) \quad V_n = \Delta_S \mu,$$

where V_n denotes the normal velocity, $\Delta_S := \nabla_S \cdot \nabla_S$ is the surface Laplace-Beltrami operator, ∇_S denotes the surface gradient with respect to the surface $S(t)$, and $\mu := \mu(\mathbf{n})$ is the chemical potential (or weighted mean curvature denoted as $H_\gamma := H_\gamma(\mathbf{n})$ in the literature) generated from the surface energy functional $W(S) := W(S(t)) =$

*Department of Mathematics, National University of Singapore, Singapore, 119076 (*mat-baowz@nus.edu.sg*). This author's research was supported by the Ministry of Education of Singapore grant MOE2019-T2-1-063 (R-146-000-296-112).

†Department of Mathematics, National University of Singapore, Singapore, 119076 (*e0444158@u.nus.edu*).

$\int_{S(t)} \gamma(\mathbf{n}) dS$ via the thermodynamic variation as $\mu = \frac{\delta W(S)}{\delta S} = \lim_{\varepsilon \rightarrow 0} \frac{W(S^\varepsilon) - W(S)}{\varepsilon}$ with S^ε being a small perturbation of S [30, 31]. It is well-known that the evolution of the surface $S(t)$ under the anisotropic surface diffusion (1.1) preserves the following two essential geometric structures [18]: (1) the volume of the region enclosed by the surface is conserved, and (2) the free surface energy (or weighted surface area) $W(S)$ decreases in time. In fact, the motion governed by the anisotropic surface diffusion can be mathematically regarded as the H^{-1} -gradient flow of the free surface energy functional (or weighted surface area) $W(S)$ [37].

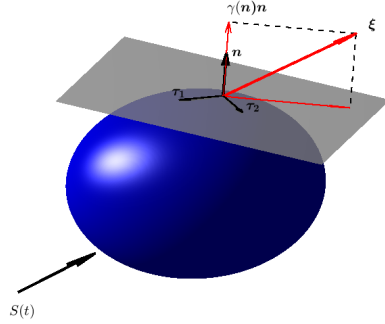


FIG. 1.1. An illustration of a closed surface $S(t)$ in \mathbb{R}^3 under anisotropic surface diffusion with an anisotropic surface energy $\gamma(\mathbf{n})$, where \mathbf{n} is the outward unit normal vector, $\boldsymbol{\xi}$ is the Cahn-Hoffman $\boldsymbol{\xi}$ -vector in (1.3), and $\boldsymbol{\tau}_1$ and $\boldsymbol{\tau}_2$ form a basis of the local tangential space.

Define $\gamma(\mathbf{p}) : \mathbb{R}_*^3 := \mathbb{R}^3 \setminus \{\mathbf{0}\} \rightarrow \mathbb{R}^+$ be a homogeneous extension of the anisotropic surface energy $\gamma(\mathbf{n}) : \mathbb{S}^2 \rightarrow \mathbb{R}^+$ satisfying: (i) $\gamma(c\mathbf{p}) = c\gamma(\mathbf{p})$ for $c > 0$ and $\mathbf{p} \in \mathbb{R}_*^3$, and (ii) $\gamma(\mathbf{p})|_{\mathbf{p}=\mathbf{n}} = \gamma(\mathbf{n})$ for $\mathbf{n} \in \mathbb{S}^2$. A typical homogeneous extension is widely used in the literature as [31, 21]

$$(1.2) \quad \gamma(\mathbf{p}) := |\mathbf{p}| \gamma\left(\frac{\mathbf{p}}{|\mathbf{p}|}\right), \quad \forall \mathbf{p} = (p_1, p_2, p_3)^T \in \mathbb{R}_*^3 := \mathbb{R}^3 \setminus \{\mathbf{0}\},$$

where $|\mathbf{p}| = \sqrt{p_1^2 + p_2^2 + p_3^2}$. Then the Cahn-Hoffman $\boldsymbol{\xi}$ -vector introduced by Cahn and Hoffman and the Hessian matrix $\mathbf{H}_\gamma(\mathbf{n})$ of $\gamma(\mathbf{p})$ are mathematically given by [28, 42]

$$(1.3) \quad \boldsymbol{\xi} = (\xi_1, \xi_2, \xi_3)^T := \boldsymbol{\xi}(\mathbf{n}) = \nabla \gamma(\mathbf{p})|_{\mathbf{p}}, \quad \mathbf{H}_\gamma(\mathbf{n}) := \nabla \nabla \gamma(\mathbf{p})|_{\mathbf{p}=\mathbf{n}}, \quad \forall \mathbf{n} \in \mathbb{S}^2.$$

Then the chemical potential μ (or weighted mean curvature) can be obtained as [17]

$$(1.4) \quad \mu = \mu(\mathbf{n}) = H_\gamma = H_\gamma(\mathbf{n}) = \nabla_S \cdot \boldsymbol{\xi} = \nabla_S \cdot \boldsymbol{\xi}(\mathbf{n}), \quad \forall \mathbf{n} \in \mathbb{S}^2.$$

For any $\mathbf{n} \in \mathbb{S}^2$, we notice that $\mathbf{H}_\gamma(\mathbf{n})\mathbf{n} = \mathbf{0}$ and thus 0 is an eigenvalue of $\mathbf{H}_\gamma(\mathbf{n})$ and \mathbf{n} is a corresponding eigenvector. We denote the other two eigenvalues of $\mathbf{H}_\gamma(\mathbf{n})$ as $\lambda_1(\mathbf{n}) \leq \lambda_2(\mathbf{n}) \in \mathbb{R}$. When $\gamma(\mathbf{n}) \equiv \text{constant}$ (e.g. $\gamma(\mathbf{n}) \equiv 1$) for $\mathbf{n} \in \mathbb{S}^2$, i.e. with isotropic surface energy, then we have $\gamma(\mathbf{p}) = |\mathbf{p}|$ in (1.2), $\boldsymbol{\xi} = \mathbf{n}$ in (1.3), and $\mu = H$ and $\mathbf{H}_\gamma(\mathbf{n}) \equiv I_3 - \mathbf{n}\mathbf{n}^T$ in (1.3) with H the mean curvature and I_3

the 3×3 identity matrix and $\lambda_1(\mathbf{n}) = \lambda_2(\mathbf{n}) \equiv 1$, and thus the anisotropic surface diffusion (1.1) collapses to the (isotropic) surface diffusion with normal velocity given as $V_n = \Delta_S H$ [9, 34]. In contrast, when $\gamma(\mathbf{n})$ is not a constant, i.e. with anisotropic surface energy: when $\boldsymbol{\tau}^T \mathbf{H}_\gamma(\mathbf{n}) \boldsymbol{\tau} > 0$ for all $\mathbf{n}, \boldsymbol{\tau} \in \mathbb{S}^2$ satisfying $\boldsymbol{\tau} \cdot \mathbf{n} := \boldsymbol{\tau}^T \mathbf{n} = 0$ ($\Leftrightarrow \lambda_2(\mathbf{n}) \geq \lambda_1(\mathbf{n}) \geq 0$ for all $\mathbf{n} \in \mathbb{S}^2$), it is called as *weakly anisotropic*; and when $\boldsymbol{\tau}^T \mathbf{H}_\gamma(\mathbf{n}) \boldsymbol{\tau}$ changes sign for $\mathbf{n}, \boldsymbol{\tau} \in \mathbb{S}^2$ satisfying $\boldsymbol{\tau} \cdot \mathbf{n} = 0$ ($\Leftrightarrow \lambda_1(\mathbf{n}) < 0$ for some $\mathbf{n} \in \mathbb{S}^2$), it is called as *strongly anisotropic*. For convenience of readers, we list several commonly-used anisotropic surface energies $\gamma(\mathbf{n})$ in the literature and their corresponding Cahn-Hoffman $\boldsymbol{\xi}$ -vectors in Appendix A.

Different numerical methods have been presented for solving the isotropic/anisotropic surface diffusion (1.1), such as the finite element method via graph evolution [3, 21], the marker-particle method [22], the discontinuous Galerkin finite element method [44], and the parametric finite element method (PFEM) [9, 12, 27, 6, 31, 32]. Among these methods, for isotropic surface diffusion, the energy-stable PFEM (ES-PFEM) based on an elegant variational formulation, which was proposed by Barrett, Garcke, and Nürnberg [9, 11] (denoted as BGN scheme), performs the best in terms of efficiency and accuracy as well as mesh quality in practical computations, especially in two dimensions (2D). The BGN scheme with unconditionally energy stability was successfully extended for solving solid-state dewetting problems with isotropic surface energy, i.e. motion of open curve and surface in 2D and 3D, respectively [9, 11]. It was also successfully extended for solving anisotropic surface diffusion Riemannian metric anisotropic surface energy [10, 12]. Recently, based on BGN's variational formulation for surface diffusion, by approximating the normal vector in a clever way, Bao and Zhao [7, 4] presented a structure-preserving PFEM (SP-PFEM) for surface diffusion, which preserves area/volume conservation in 2D/3D and unconditionally energy dissipation in the discretized level. Very recently, by introducing a proper surface energy matrix depending on the Cahn-Hoffman $\boldsymbol{\xi}$ -vector and a stabilizing function, we obtained a new symmetrized (and conservative) variational formulation for anisotropic surface diffusion with arbitrary surface energy in 2D and then designed structure-preserving and energy-stable PFEM under mild and simple conditions on the surface energy [5]. The main aim of this paper is to extend the above method from 2D to 3D for anisotropic surface diffusion with arbitrary surface energy. Again, the key is based on introducing a proper surface energy matrix depending on the Cahn-Hoffman $\boldsymbol{\xi}$ -vector and a stabilizing function in 3D and obtaining a new symmetrized (and conservative) variational formulation. The difficulty and major part is to establish unconditionally energy dissipation of the full discretization under the following simple and mild condition on the arbitrary surface energy $\gamma(\mathbf{n})$ as

$$(1.5) \quad \gamma(-\mathbf{n}) = \gamma(\mathbf{n}), \quad \forall \mathbf{n} \in \mathbb{S}^2, \quad \gamma(\mathbf{p}) \in C^2(\mathbb{R}^3 \setminus \{\mathbf{0}\}).$$

The paper is organized as follows. In section 2, we recall the mathematical representations for anisotropic surface diffusion, obtain a symmetrized variational formulation and propose a SP-FEM to discretize it. In section 3, we establish energy stability of the proposed SP-PFEM. Extensive numerical results are reported to demonstrate the efficiency and accuracy as well as structure-preserving properties in section 4. Finally, some conclusions are drawn in section 5.

2. A new symmetrized variational formulation and its discretization.

This section first discusses the mathematical representations for the anisotropic surface diffusion. Then to introduce the weak formulation of μ in 3D, we generalize the surface energy matrix $\mathbf{Z}_k(\mathbf{n})$ for 2D anisotropic surface diffusion into 3D. A sym-

metrized conservative variational formulation for anisotropic surface diffusion in 3D is then derived by using the weak formulation and the surface energy matrix $\mathbf{Z}_k(\mathbf{n})$, and we show the two geometric properties are preserved for the new symmetrized variational formulation. Finally, by adopting backward Euler in time and the parametric finite element method in space, we derive the full discretization for the variational formulation and establish its structural preserving properties.

2.1. Mathematical representations for anisotropic surface diffusion. Let the closed surface $S := S(t)$ be parameterized by $\mathbf{X}(\boldsymbol{\rho}, t)$ as

$$(2.1) \quad \mathbf{X}(t) : \Omega \rightarrow \mathbb{R}^3, \boldsymbol{\rho} \mapsto \mathbf{X}(\boldsymbol{\rho}, t) = (X_1(\boldsymbol{\rho}, t), X_2(\boldsymbol{\rho}, t), X_3(\boldsymbol{\rho}, t))^T,$$

where $\Omega \subset \mathbb{R}^2$, then the motion of $S(t)$ under the anisotropic surface diffusion (1.1) can be mathematically described by the following geometric partial differential equations via the Cahn-Hoffman $\boldsymbol{\xi}$ -vector as [21]

$$(2.2a) \quad \begin{cases} \partial_t \mathbf{X}(\boldsymbol{\rho}, t) = (\Delta_S \mu) \mathbf{n}, & \boldsymbol{\rho} \in \Omega, \quad t > 0, \\ \mu = \nabla_S \cdot \boldsymbol{\xi}, & \boldsymbol{\xi} = \nabla \gamma(\mathbf{p})|_{\mathbf{p}=\mathbf{n}}. \end{cases}$$

The anisotropic surface diffusion (2.2) can also be regarded as a geometric flow from the given initial closed surface $S_0 := S(0) \subset \mathbb{R}^3$ to the surface $S(t) \subset \mathbb{R}^3$. We define the function spaces over the evolving surface $S(t) = \mathbf{X}(\boldsymbol{\rho}, t)$.

$$(2.3) \quad L^2(S(t)) := \left\{ u : S(t) \rightarrow \mathbb{R} \mid \int_{S(t)} |u|^2 dA < \infty \right\},$$

equipped with the L^2 -inner product

$$(2.4) \quad (u, v)_{S(t)} := \int_{S(t)} u v dA, \quad \forall u, v \in L^2(S(t)),$$

here dA is the surface measure. This inner product can be extend to $[L^2(S(t))]^3$ by replacing the scalar product $u v$ by the vector inner product $\mathbf{u} \cdot \mathbf{v}$. And we adopt the angle bracket to emphasize the inner product for two matrix-valued functions \mathbf{U}, \mathbf{V} in $[L^2(S(t))]^{3 \times 3}$,

$$(2.5) \quad \langle \mathbf{U}, \mathbf{V} \rangle_{S(t)} := \int_{S(t)} \mathbf{U} : \mathbf{V} dA, \quad \forall \mathbf{U}, \mathbf{V} \in [L^2(S(t))]^{3 \times 3},$$

here $\mathbf{U} : \mathbf{V} = \text{Tr}(\mathbf{V}^T \mathbf{U})$ is the Frobenius inner product. Furthermore, we introduce the Sobolev space

$$(2.6) \quad H^1(S(t)) := \left\{ u : S(t) \rightarrow \mathbb{R} \mid u \in L^2(S(t)), \nabla_S u \in [L^2(S(t))]^3 \right\}.$$

And this definition is also valid for the function in $[H^1(S(t))]^3$.

We refer to the definition of surface gradient ∇_S for scalar-valued functions [21]. And the surface gradient for a vector-valued function $\mathbf{F} = (F_1, F_2, F_3)^T$ is defined as

$$(2.7) \quad \nabla_S \mathbf{F} := (\nabla_S F_1, \nabla_S F_2, \nabla_S F_3)^T \in \mathbb{R}^{3 \times 3}.$$

2.2. A new symmetrized variational formulation and its property. First, we generalize the 2D symmetric surface energy matrix $\mathbf{Z}_k(\mathbf{n})$ proposed in [5] into 3D by

$$(2.8) \quad \mathbf{Z}_k(\mathbf{n}) = \gamma(\mathbf{n})I_3 - \mathbf{n}\boldsymbol{\xi}^T(\mathbf{n}) - \boldsymbol{\xi}(\mathbf{n})\mathbf{n}^T + k(\mathbf{n})\mathbf{n}\mathbf{n}^T, \quad \forall \mathbf{n} \in \mathbb{S}^2,$$

where I_3 is the 3×3 identity matrix, $k(\mathbf{n})$ is the stabilizing function which ensures $\mathbf{Z}_k(\mathbf{n})$ is positive definite.

We then show this generalization of $\mathbf{Z}_k(\mathbf{n})$ is reasonable by showing the strong formulation $\mu\mathbf{n} = -\partial_s(\mathbf{Z}_k(\mathbf{n})\partial_s\mathbf{X})$ introduced in [5] for the weighted mean curvature μ in 2D can be generalized to the following weak formulation in 3D.

LEMMA 2.1 (The weak formulation for μ). *The weighted mean curvature μ satisfies the following weak formulation.*

$$(2.9) \quad (\mu, \mathbf{n} \cdot \boldsymbol{\omega})_S = \langle \mathbf{Z}_k(\mathbf{n})\nabla_S\mathbf{X}, \nabla_S\boldsymbol{\omega} \rangle_S,$$

where $\boldsymbol{\omega} = (\omega_1, \omega_2, \omega_3)^T : S \rightarrow \mathbb{R}^3$ is a smooth test function.

Proof. We adopt the notation $\nabla_S f = (\underline{D}_1 f, \underline{D}_2 f, \underline{D}_3 f)^T$. Noticing the fact $\underline{D}_i X_k = \delta_{i,k} - n_k n_i$ and $\nabla_S f \cdot \mathbf{n} = 0$, we obtain

$$(2.10) \quad \nabla_S X_k \cdot \nabla_S \omega_l = \sum_{i=1}^3 (\delta_{i,k} - n_k n_i) \underline{D}_i \omega_l = \underline{D}_k \omega_l - n_k \nabla_S \omega_l \cdot \mathbf{n} = \underline{D}_k \omega_l.$$

Substitute the identity (2.10) in [21, equation (8.18)] yields the following identity

$$(2.11) \quad (\mu, \mathbf{n} \cdot \boldsymbol{\omega})_S = \gamma(\mathbf{n}) \sum_{l=1}^3 \int_S \nabla_S X_l \cdot \nabla_S \omega_l dA - \sum_{k,l=1}^3 \int_S \xi_k n_l \nabla_S X_k \cdot \nabla_S \omega_l dA.$$

Obviously, the second term $\langle \gamma(\mathbf{n})\nabla_S\mathbf{X}, \nabla_S\boldsymbol{\omega} \rangle_S$ corresponds to $\gamma(\mathbf{n})I_3$ in $\mathbf{Z}_k(\mathbf{n})$. Now by simplifying the last term, we have

$$\begin{aligned} \sum_{k,l=1}^3 \int_S \xi_k n_l \nabla_S X_k \cdot \nabla_S \omega_l dA &= \int_S \left(\sum_{k=1}^3 \xi_k (\nabla_S X_k) \right) \cdot \left(\sum_{l=1}^3 n_l (\nabla_S \omega_l) \right) dA \\ &= \int_S ((\nabla_S \mathbf{X})^T \boldsymbol{\xi}) \cdot ((\nabla_S \boldsymbol{\omega})^T \mathbf{n}) dA \\ &= \int_S \text{Tr} \left((\nabla_S \boldsymbol{\omega})^T \mathbf{n} \boldsymbol{\xi}^T (\nabla_S \mathbf{X}) \right) dA \\ &= \int_S \left(\mathbf{n} \boldsymbol{\xi}^T (\nabla_S \mathbf{X}) \right) : (\nabla_S \boldsymbol{\omega}) dA \\ (2.12) \quad &= \langle \mathbf{n} \boldsymbol{\xi}^T \nabla_S \mathbf{X}, \nabla_S \boldsymbol{\omega} \rangle_S, \end{aligned}$$

which is the $\mathbf{n}\boldsymbol{\xi}^T(\mathbf{n})$ part in $\mathbf{Z}_k(\mathbf{n})$.

Finally, recall the identity $\nabla_S \mathbf{X} = I_3 - \mathbf{n}\mathbf{n}^T$ and combine the two identities (2.11) and (2.12) yields

$$\begin{aligned} (\mu, \mathbf{n} \cdot \boldsymbol{\omega})_S &= \langle (\gamma(\mathbf{n})I_3 - \mathbf{n}\boldsymbol{\xi}^T) \nabla_S \mathbf{X}, \nabla_S \boldsymbol{\omega} \rangle_S \\ &= \langle \mathbf{Z}_k(\mathbf{n}) \nabla_S \mathbf{X}, \nabla_S \boldsymbol{\omega} \rangle_S + \langle (\boldsymbol{\xi} \mathbf{n}^T - k(\mathbf{n})\mathbf{n}\mathbf{n}^T)(I_3 - \mathbf{n}\mathbf{n}^T), \nabla_S \boldsymbol{\omega} \rangle_S \\ (2.13) \quad &= \langle \mathbf{Z}_k(\mathbf{n}) \nabla_S \mathbf{X}, \nabla_S \boldsymbol{\omega} \rangle_S, \end{aligned}$$

which is the desired result. \square

With the weak formulation of μ (2.9) given in lemma 2.1, by taking integration by parts, we can easily derive the following variational formulation for the anisotropic surface diffusion (1.1). For a given closed initial surface $S(0) := S_0$, find the solution $(\mathbf{X}(\cdot, t), \mu(\cdot, t)) \in [H^1(S(t))]^3 \times H^1(S(t))$ such that

$$(2.14a) \quad (\partial_t \mathbf{X} \cdot \mathbf{n}, \psi)_{S(t)} + (\nabla_S \mu, \nabla_S \psi)_{S(t)} = 0 \quad \forall \psi \in H^1(S(t)),$$

$$(2.14b) \quad (\mu \mathbf{n}, \boldsymbol{\omega})_{S(t)} - \langle Z_k(\mathbf{n}) \nabla_S \mathbf{X}, \nabla_S \boldsymbol{\omega} \rangle_{S(t)} = 0 \quad \forall \boldsymbol{\omega} \in [H^1(S(t))]^3,$$

Denote the enclosed volume and the free energy of $S(t)$ as $V(t)$ and $W(t)$, respectively, which are defined by

$$(2.15) \quad V(t) := \frac{1}{3} \int_{S(t)} \mathbf{X} \cdot \mathbf{n} dA, \quad W(t) := \int_{S(t)} \gamma(\mathbf{n}) dA.$$

We then show the two geometric properties still hold for the variational formulation (2.14).

THEOREM 2.2. *The enclosed volume $V(t)$ and the free energy $W(t)$ of the solution $S(t)$ of the variational formulation (2.14) are conserved and dissipative, respectively.*

Proof. Taking the derivative of $V(t)$ with respect to t . From [38], we know that

$$(2.16) \quad \frac{dV(t)}{dt} = \int_{S(t)} V_n dA = (\partial_t \mathbf{X} \cdot \mathbf{n}, 1)_{S(t)} = 0.$$

Similarly, the derivative of $W(t)$ with respect to t is

$$(2.17) \quad \frac{dW(t)}{dt} = \int_{S(t)} V_n \mu dA = (\partial_t \mathbf{X} \cdot \mathbf{n}, \mu)_{S(t)} = -(\nabla_S \mu, \nabla_S \mu)_{S(t)},$$

which means $\frac{dW(t)}{dt} \leq 0$. \square

2.3. A structural-preserving parametric finite element method. We take $\tau > 0$ to be the time step size, and the discrete time levels are $t_m = m\tau$ for each $m \geq 0$. For spatial discretization, as illustrated in figure 2.1, the surface $S(t_m)$ is approximated by a polyhedron $S^m = \cup_{j=1}^J \bar{\sigma}_j^m$ with J mutually disjoint non-degenerated triangles surfaces σ_j^m and I vertices \mathbf{q}_i^m . We further denote $\{\mathbf{q}_{j_1}^m, \mathbf{q}_{j_2}^m, \mathbf{q}_{j_3}^m\}$ as the three counterclockwise vertices of the triangle σ_j^m , and $\mathcal{J}\{\sigma_j^m\} := (\mathbf{q}_{j_2}^m - \mathbf{q}_{j_1}^m) \times (\mathbf{q}_{j_3}^m - \mathbf{q}_{j_1}^m)$ is the orientation vector with respect to σ_j^m , and the outward unit normal vector \mathbf{n}_j^m of σ_j^m is thus given by $\mathbf{n}_j^m = \frac{\mathcal{J}\{\sigma_j^m\}}{|\mathcal{J}\{\sigma_j^m\}|}$.

The finite element space with respect to the surface $S^m = \cup_{j=1}^J \bar{\sigma}_j^m$ is defined as follows

$$(2.18) \quad \mathbb{K}^m := \left\{ u \in C(S^m) \mid u|_{\sigma_j^m} \in \mathcal{P}^1(\sigma_j^m), \forall 1 \leq j \leq J \right\},$$

equipped with the mass lumped inner product $(\cdot, \cdot)_{S^m}$ as

$$(2.19) \quad (f, g)_{S^m} := \frac{1}{3} \sum_{j=1}^J \sum_{i=1}^3 |\sigma_j^m| f((\mathbf{q}_{j_i}^m)^-) g((\mathbf{q}_{j_i}^m)^-).$$

Where $\mathcal{P}^1(\sigma_j^m)$ is the space of polynomials on σ_j^m with degree at almost 1, $|\sigma_j^m| := \frac{1}{2} |\mathcal{J}\{\sigma_j^m\}|$ denotes the area of σ_j^m , and $f((\mathbf{q}_{j_i}^m)^-)$ means the one-sided limit of $f(x)$

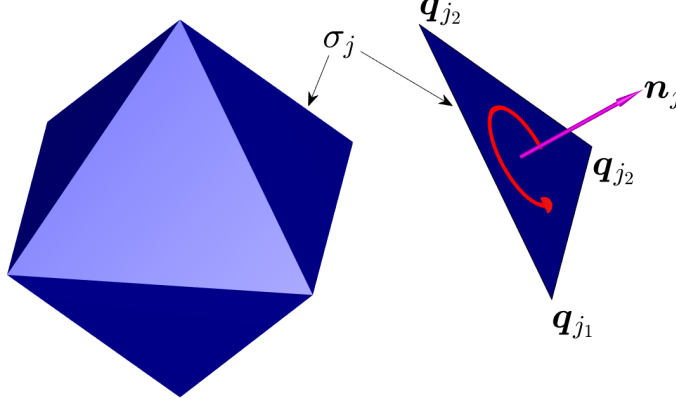


FIG. 2.1. An illustration of the approximation polyhedron S^0 . The vertices $\{q_{j1}, q_{j2}, q_{j3}\}$ of the triangle σ_j is oriented counterclockwise, see the red circular arrow. And the direction of the normal vector \mathbf{n}_j is determined by the right-hand rule.

at $\mathbf{q}_{j_i}^m$ inside σ_j^m . This definition is also valid for vector- and matrix-valued function, and the inner product of the matrix-valued functions \mathbf{U} and \mathbf{V} is also emphasized by the angle bracket as

$$(2.20) \quad \langle \mathbf{U}, \mathbf{V} \rangle_{S^m} := \frac{1}{3} \sum_{j=1}^J \sum_{i=1}^3 |\sigma_j^m| \mathbf{U}((\mathbf{q}_{j_i}^m)^-) : \mathbf{V}((\mathbf{q}_{j_i}^m)^-).$$

Finally, the discretized surface gradient operator ∇_S for $f \in \mathbb{K}^m$ is given by

$$(2.21) \quad \nabla_S f|_{\sigma_j^m} := \left(f(\mathbf{q}_{j1}^m)(\mathbf{q}_{j2}^m - \mathbf{q}_{j3}^m) + f(\mathbf{q}_{j2}^m)(\mathbf{q}_{j3}^m - \mathbf{q}_{j1}^m) + f(\mathbf{q}_{j3}^m)(\mathbf{q}_{j1}^m - \mathbf{q}_{j2}^m) \right) \times \frac{\mathbf{n}_j^m}{|\mathcal{J}\{\sigma_j^m\}|},$$

and for vector-valued function $\mathbf{F} = (F_1, F_2, F_3)^T \in [\mathbb{K}^m]^3$, $\nabla_S \mathbf{F} := (\nabla_S F_1, \nabla_S F_2, \nabla_S F_3)^T$.

The full-implicit structural-preserving finite element method (SP-PFEM) for the variational formulation (2.14) can then be stated as follows: given the initial approximation $S^0 = \cup_{j=1}^J \bar{\sigma}_j^0$ of $S(0)$. For each time step $t_m = m\tau$, $m = 0, 1, 2, \dots$, find the solution $(\mathbf{X}^{m+1}, \mu^{m+1}) \in [\mathbb{K}^m]^3 \times \mathbb{K}^m$ such that

$$(2.22a) \quad \left(\frac{\mathbf{X}^{m+1} - \mathbf{X}^m}{\tau} \cdot \mathbf{n}^{m+\frac{1}{2}}, \psi \right)_{S^m} + (\nabla_S \mu^{m+1}, \nabla_S \psi)_{S^m} = 0, \quad \forall \psi \in \mathbb{K}^m,$$

$$(2.22b) \quad \left(\mu^{m+1} \mathbf{n}^{m+\frac{1}{2}}, \boldsymbol{\omega} \right)_{S^m} - \langle \mathbf{Z}_k(\mathbf{n}^m) \nabla_S \mathbf{X}^{m+1}, \nabla_S \boldsymbol{\omega} \rangle_{S^m} = 0, \quad \forall \boldsymbol{\omega} \in [\mathbb{K}^m]^3.$$

Here $\mathbf{X}^m(\mathbf{q}_i^m) = \mathbf{q}_i^m$, $\mathbf{X}^{m+1}(\mathbf{q}_i^m) = \mathbf{q}_i^{m+1}$ for each i , $\mathbf{n}^m|_{\sigma_j^m} = \mathbf{n}_j^m$, $\sigma_j^{m+1} = \mathbf{X}^{m+1}(\sigma_j^m)$ is the triangle with counterclockwise ordered vertices $\{\mathbf{q}_{j1}^{m+1}, \mathbf{q}_{j2}^{m+1}, \mathbf{q}_{j3}^{m+1}\}$

for each j , and $S^{m+1} = \cup_{j=1}^J \bar{\sigma}_j^{m+1}$ for each m . The semi-implicit approximation $\mathbf{n}^{m+\frac{1}{2}}$ of the outward normal vector \mathbf{n} at $t = (m + \frac{1}{2})\tau$ is defined as follows

$$(2.23) \quad \mathbf{n}^{m+\frac{1}{2}}|_{\sigma_j^m} := \frac{\mathcal{J}\{\sigma_j^m\} + 4\mathcal{J}\{\sigma_j^{m+\frac{1}{2}}\} + \mathcal{J}\{\sigma_j^{m+1}\}}{6|\mathcal{J}\{\sigma_j^m\}|},$$

where $\sigma_j^{m+\frac{1}{2}} := \frac{1}{2}(\sigma_j^m + \sigma_j^{m+1})$.

REMARK 2.1. We note the function \mathbf{X}^{m+1} has different meanings at time step t_m (as a function in $[\mathbb{K}^m]^3$) and t_{m+1} (as a function in $[\mathbb{K}^{m+1}]^3$), and we adopt the same notation for simplicity.

2.4. Main results. For the discretized polygon surface $S^m = \cup_{j=1}^J \bar{\sigma}_j^m$, its enclosed volume and surface energy are denoted as V^m and W^m , respectively, which are defined as

$$(2.24a) \quad V^m := \frac{1}{3} \int_{S^m} \mathbf{X}^m \cdot \mathbf{n}^m dA = \frac{1}{9} \sum_{j=1}^J \sum_{i=1}^3 |\sigma_j^m| \mathbf{q}_{ji}^m \cdot \mathbf{n}_j^m,$$

$$(2.24b) \quad W^m := \int_{S^m} \gamma(\mathbf{n}^m) dA = \sum_{j=1}^J |\sigma_j^m| \gamma(\mathbf{n}_j^m), \quad \forall m \geq 0.$$

Denote the following axillary function $F_k(\mathbf{n}, \mathbf{u}, \mathbf{v}) : [\mathbb{S}^2]^3 \rightarrow \mathbb{R}$ as

$$(2.25) \quad F_k(\mathbf{n}, \mathbf{u}, \mathbf{v}) := (\mathbf{u}^T \mathbf{Z}_k(\mathbf{n}) \cdot \mathbf{u})(\mathbf{v}^T \mathbf{Z}_k(\mathbf{n}) \cdot \mathbf{v}),$$

and define the minimal stabilizing function $k_0(\mathbf{n}) : \mathbb{S}^2 \rightarrow \mathbb{R}$ as (its existence will be given in next section)

$$(2.26) \quad k_0(\mathbf{n}) = \inf \left\{ k(\mathbf{n}) \mid F_k(\mathbf{n}, \mathbf{u}, \mathbf{v}) \geq \gamma^2(\mathbf{u} \times \mathbf{v}), \quad \forall \mathbf{u}, \mathbf{v} \in \mathbb{S}^2 \right\}.$$

Then for the SP-PFEM (2.22), we have

THEOREM 2.3 (structural-preserving). Assume $\gamma(\mathbf{n})$ satisfies (1.5) and take $k(\mathbf{n})$ in (2.8) satisfying $k(\mathbf{n}) \geq k_0(\mathbf{n})$ for $\mathbf{n} \in \mathbb{S}^2$, then the SP-PFEM (2.22) is volume conservation and energy dissipation, i.e.

$$(2.27a) \quad V^{m+1} = V^m = \dots = V^0, \quad \forall m \geq 0,$$

$$(2.27b) \quad W^{m+1} \leq W^m \leq \dots \leq W^0, \quad \forall m \geq 0.$$

The proof of volume conservation (2.27a) is similar to [8] and thus it is omitted here for brevity, and we will establish the energy dissipation or unconditional energy stability (2.27b) in next section.

REMARK 2.2. The semi-discretization of the variational form (2.14) also preserves the two geometric properties. And the proof is similar to the isotropic case; we refer [9, 46, 8] for the result of semi-discretization of 3D isotropic surface diffusion.

3. Energy stability. In this section, we first prove the existence of $k_0(\mathbf{n})$ and show its sub-linear property as a functional of $\gamma(\mathbf{n})$. By utilizing the existence of $k_0(\mathbf{n})$ together with several lemmas, we finally prove the energy stability part of our main theorem (2.27b).

3.1. Minimal stabilizing function. From (2.26), we know that $F_{k_0}(\mathbf{n}, \mathbf{u}, \mathbf{v}) \geq 0$. Take $\mathbf{u} = \mathbf{n}$ in (2.25), it yields $k_0(\mathbf{n}) - \gamma(\mathbf{n}) \geq 0$, and we have a finite lower bound for $k_0(\mathbf{n})$. To prove the existence of $k_0(\mathbf{n})$, we only need to show $k_0(\mathbf{n}) < \infty$, and this is given by the following upper bound estimation of $k_0(\mathbf{n})$. And we begin with the following lemma.

LEMMA 3.1. *Let $G(\mathbf{n}, \mathbf{u}, \mathbf{v})$ be an auxillary function given by*

$$(3.1) \quad G(\mathbf{n}, \mathbf{u}, \mathbf{v}) := \gamma(\mathbf{n}) (\gamma(\mathbf{n}) - 2(\boldsymbol{\xi} \cdot \mathbf{u})(\mathbf{n} \cdot \mathbf{u}) - 2(\boldsymbol{\xi} \cdot \mathbf{v})(\mathbf{n} \cdot \mathbf{v})),$$

then for any $k(\mathbf{n}) > 0$, the following inequality holds

$$(3.2) \quad F_k(\mathbf{n}, \mathbf{u}, \mathbf{v}) - G(\mathbf{n}, \mathbf{u}, \mathbf{v}) \geq (\gamma(\mathbf{n})k(\mathbf{n}) - 4|\boldsymbol{\xi}|^2) ((\mathbf{n} \cdot \mathbf{u})^2 + (\mathbf{n} \cdot \mathbf{v})^2).$$

Proof. By direct computation and the arithmetic-geometric mean inequality, we obtain

$$\begin{aligned} & F_k(\mathbf{n}, \mathbf{u}, \mathbf{v}) - G(\mathbf{n}, \mathbf{u}, \mathbf{v}) \\ & \geq \gamma(\mathbf{n})k(\mathbf{n}) ((\mathbf{n} \cdot \mathbf{u})^2 + (\mathbf{n} \cdot \mathbf{v})^2) + k(\mathbf{n})^2(\mathbf{n} \cdot \mathbf{u})^2(\mathbf{n} \cdot \mathbf{v})^2 \\ & \quad - 4|\boldsymbol{\xi}|^2 |(\mathbf{n} \cdot \mathbf{u})(\mathbf{n} \cdot \mathbf{v})| - 2|\boldsymbol{\xi}|k(\mathbf{n}) |(\mathbf{n} \cdot \mathbf{u})(\mathbf{n} \cdot \mathbf{v})| (|(\mathbf{n} \cdot \mathbf{u})| + |(\mathbf{n} \cdot \mathbf{v})|) \\ & \geq (\gamma(\mathbf{n})k(\mathbf{n}) - 2|\boldsymbol{\xi}|^2) ((\mathbf{n} \cdot \mathbf{u})^2 + (\mathbf{n} \cdot \mathbf{v})^2) + k(\mathbf{n})^2(\mathbf{n} \cdot \mathbf{u})^2(\mathbf{n} \cdot \mathbf{v})^2 \\ & \quad - k(\mathbf{n})|\boldsymbol{\xi}| \left((\mathbf{n} \cdot \mathbf{u})^2 \left(\frac{2|\boldsymbol{\xi}|}{k(\mathbf{n})} + \frac{k(\mathbf{n})}{2|\boldsymbol{\xi}|} (\mathbf{n} \cdot \mathbf{v})^2 \right) + (\mathbf{n} \cdot \mathbf{v})^2 \left(\frac{2|\boldsymbol{\xi}|}{k(\mathbf{n})} + \frac{k(\mathbf{n})}{2|\boldsymbol{\xi}|} (\mathbf{n} \cdot \mathbf{u})^2 \right) \right) \\ & = (\gamma(\mathbf{n})k(\mathbf{n}) - 4|\boldsymbol{\xi}|^2) ((\mathbf{n} \cdot \mathbf{u})^2 + (\mathbf{n} \cdot \mathbf{v})^2), \end{aligned}$$

which is the desired inequality. \square

Since $\gamma(\mathbf{n})$ is not differentiable at $\mathbf{0}$, the cross product $\gamma^2(\mathbf{u} \times \mathbf{v}) \notin C^2(\mathbb{S}^2 \times \mathbb{S}^2)$. The following lemma is helpful in estimating $\gamma^2(\mathbf{u} \times \mathbf{v})$,

LEMMA 3.2. *For any $\gamma(\mathbf{n})$ satisfying (1.5), i.e., $\gamma(\mathbf{n}) \in C^2(\mathbb{S}^2)$ with $\gamma(-\mathbf{n}) = \gamma(\mathbf{n})$, $\gamma^2(\mathbf{p})$ is continuous differentiable in \mathbb{R}^3 . Moreover, there exists a constant C_1 defined by*

$$(3.3) \quad C_1 = \frac{1}{2} \sup_{\mathbf{n} \in \mathbb{S}^2} \|\mathbf{H}_{\gamma^2}(\mathbf{n})\|_2,$$

such that

$$(3.4) \quad \gamma^2(\mathbf{p}) - \gamma^2(\mathbf{q}) \leq \nabla(\gamma^2(\mathbf{q})) \cdot (\mathbf{p} - \mathbf{q}) + C_1 |\mathbf{p} - \mathbf{q}|^2, \quad \forall \mathbf{p}, \mathbf{q} \in \mathbb{R}^3.$$

Where $\|\cdot\|_2$ is the spectral norm.

Proof. It's straitforward to check $\gamma^2(\mathbf{p})$ is continuous differentiable by definition. To prove the inequality (3.4), we first consider the case the line segment of \mathbf{p}, \mathbf{q} does not pass $\mathbf{0}$, i.e., $\lambda \mathbf{p} + (1 - \lambda) \mathbf{q} \neq \mathbf{0}, \forall 0 \leq \lambda \leq 1$. Since $\gamma^2(\mathbf{p})$ is homogeneous of degree 2, we know that $\mathbf{H}_{\gamma^2}(\mathbf{p})$ is homogeneous of degree 0, which yields

$$(3.5) \quad \mathbf{H}_{\gamma^2}(\boldsymbol{\zeta}) = \mathbf{H}_{\gamma^2}(\boldsymbol{\zeta}/|\boldsymbol{\zeta}|), \quad \forall \boldsymbol{\zeta} \neq \mathbf{0}.$$

By mean value theorem, there exists a $\lambda_0 \in (0, 1)$ and $\boldsymbol{\zeta} = \lambda_0 \mathbf{p} + (1 - \lambda_0) \mathbf{q} \neq \mathbf{0}$, such that

$$(3.6) \quad \gamma^2(\mathbf{p}) = \gamma^2(\mathbf{q}) + \nabla(\gamma^2(\mathbf{q})) \cdot (\mathbf{p} - \mathbf{q}) + \frac{1}{2} (\mathbf{p} - \mathbf{q})^T \mathbf{H}_{\gamma^2}(\boldsymbol{\zeta}) \cdot (\mathbf{p} - \mathbf{q}).$$

Thus (3.4) holds for such \mathbf{p}, \mathbf{q} .

If $\mathbf{0}$ is contained in line segment of \mathbf{p}, \mathbf{q} , we can find a sequence $(\mathbf{p}_k, \mathbf{q}_k) \rightarrow (\mathbf{p}, \mathbf{q})$ such that for each k , the line segment of $\mathbf{p}_k, \mathbf{q}_k$ does not pass $\mathbf{0}$. We know (3.4) holds for such $\mathbf{p}_k, \mathbf{q}_k$. And the (3.4) is thus valid for all \mathbf{p}, \mathbf{q} by the continuity of $\gamma^2(\mathbf{p})$ and $\nabla(\gamma^2(\mathbf{p}))$. \square

THEOREM 3.3. *Suppose $\gamma(\mathbf{n})$ satisfies the energy stable condition (1.5). Then there exists a constant $K(\mathbf{n}) < \infty$ only depends on $\gamma(\mathbf{n})$ given by*

$$(3.7) \quad K(\mathbf{n}) = \frac{6|\boldsymbol{\xi}|^2 + 8\gamma(\mathbf{n})|\boldsymbol{\xi}| + 16C_1}{\gamma(\mathbf{n})} < \infty,$$

such that $F_K(\mathbf{n}, \mathbf{u}, \mathbf{v}) \geq \gamma^2(\mathbf{u} \times \mathbf{v})$, $\forall \mathbf{u}, \mathbf{v} \in \mathbb{S}^2$.

Proof. It is convenient to consider the special case $\mathbf{n} = (0, 0, 1)^T$. We write \mathbf{u}, \mathbf{v} in the spherical coordinates,

$$(3.8a) \quad \mathbf{u} = (\cos \phi_1 \cos \theta_1, \cos \phi_1 \sin \theta_1, \sin \phi_1)^T,$$

$$(3.8b) \quad \mathbf{v} = (\cos \phi_2 \cos \theta_2, \cos \phi_2 \sin \theta_2, \sin \phi_2)^T,$$

where $-\frac{\pi}{2} \leq \phi_1, \phi_2 \leq \frac{\pi}{2}$, $0 \leq \theta_1, \theta_2 < 2\pi$. And in case $\phi = \pm \frac{\pi}{2}$, we choose $\theta = 0$. The cross product $\mathbf{u} \times \mathbf{v}$ is then represented as

$$(3.9) \quad \mathbf{u} \times \mathbf{v} = \cos \phi_2 \sin \phi_1 \hat{\mathbf{v}}_0 + \cos \phi_1 \sin \phi_2 \hat{\mathbf{u}}_0 + \cos \phi_1 \cos \phi_2 (0, 0, \sin \theta_{2,1})^T,$$

where

$$(3.10) \quad \hat{\mathbf{u}}_0 = (\sin \theta_1, -\cos \theta_1, 0)^T, \quad \hat{\mathbf{v}}_0 = (-\sin \theta_2, \cos \theta_2, 0)^T, \quad \theta_{2,1} = \theta_2 - \theta_1.$$

And denote $\mathbf{u}_0, \mathbf{v}_0$ as

$$(3.11) \quad \mathbf{u}_0 := (\cos \theta_1, \sin \theta_1, 0)^T, \quad \mathbf{v}_0 := (\cos \theta_2, \sin \theta_2, 0)^T.$$

Since $|\mathbf{u}|, |\mathbf{v}|, |\mathbf{u}_0|, |\mathbf{v}_0| = 1$, we know that $|(\mathbf{u} - \mathbf{u}_0) \times \mathbf{v}| \leq |\mathbf{u} - \mathbf{u}_0|, |\mathbf{u} \times (\mathbf{v} - \mathbf{v}_0)| \leq |\mathbf{v} - \mathbf{v}_0|, |(\mathbf{u} - \mathbf{u}_0) \times (\mathbf{v} - \mathbf{v}_0)| \leq |\mathbf{u} - \mathbf{u}_0| + |\mathbf{v} - \mathbf{v}_0|$, and thus

$$(3.12) \quad |\mathbf{u} \times \mathbf{v} - \mathbf{u}_0 \times \mathbf{v}_0|^2 \leq 8(|\mathbf{u} - \mathbf{u}_0|^2 + |\mathbf{v} - \mathbf{v}_0|^2).$$

By taking $\mathbf{p} = \mathbf{u} \times \mathbf{v}, \mathbf{q} = \mathbf{u}_0 \times \mathbf{v}_0$ in (3.4), and noticing $\mathbf{u}_0 \times \mathbf{v}_0 = (\sin \theta_{2,1}) \mathbf{n}$, we obtain

$$(3.13) \quad \begin{aligned} & \gamma^2(\mathbf{u} \times \mathbf{v}) - (\sin \Delta\theta)^2 \gamma^2(\mathbf{n}) \\ & \leq \sin \theta_{2,1} \nabla(\gamma^2(\mathbf{n})) \cdot (\mathbf{u} \times \mathbf{v} - \mathbf{u}_0 \times \mathbf{v}_0) + C_1 |\mathbf{u} \times \mathbf{v} - \mathbf{u}_0 \times \mathbf{v}_0|^2 \\ & \leq 2\gamma(\mathbf{n}) \boldsymbol{\xi} \cdot (\sin \phi_1 \hat{\mathbf{v}}_0 + \sin \phi_2 \hat{\mathbf{u}}_0) \sin \theta_{2,1} \\ & \quad + 4\gamma(\mathbf{n}) |\boldsymbol{\xi}| ((\sin \phi_1)^2 + (\sin \phi_2)^2) + 8C_1 (|\mathbf{u} - \mathbf{u}_0|^2 + |\mathbf{v} - \mathbf{v}_0|^2) \\ & \leq 2\gamma(\mathbf{n}) \boldsymbol{\xi} \cdot ((\cos \theta_{2,1} \mathbf{v}_0 - \mathbf{u}_0) (\mathbf{n} \cdot \mathbf{u}) + (\cos \theta_{2,1} \mathbf{u}_0 - \mathbf{v}_0) (\mathbf{n} \cdot \mathbf{v})) \\ & \quad + 4(\gamma(\mathbf{n}) |\boldsymbol{\xi}| + 4C_1) ((\mathbf{n} \cdot \mathbf{u})^2 + (\mathbf{n} \cdot \mathbf{v})^2). \end{aligned}$$

Where we use the facts $|\mathbf{u} - \mathbf{u}_0| = 2|\sin \frac{\phi_1}{2}|, |\mathbf{v} - \mathbf{v}_0| = 2|\sin \frac{\phi_2}{2}|$ and $(\sin \phi)^2 \geq 2(\sin \frac{\phi}{2})^2 = 1 - \cos \phi, \forall -\frac{\pi}{2} \leq \phi \leq \frac{\pi}{2}$.

To estimate $G(\mathbf{n}, \mathbf{u}, \mathbf{v})$, we observe the following inequalities

$$(3.14a) \quad \begin{aligned} (\boldsymbol{\xi} \cdot \mathbf{u})(\mathbf{n} \cdot \mathbf{u}) &= (\boldsymbol{\xi} \cdot \mathbf{u}_0)(\mathbf{n} \cdot \mathbf{u}) + (\boldsymbol{\xi} \cdot (\mathbf{u} - \mathbf{u}_0))(\mathbf{n} \cdot (\mathbf{u} - \mathbf{u}_0)) \\ &\geq (\boldsymbol{\xi} \cdot \mathbf{u}_0)(\mathbf{n} \cdot \mathbf{u}) - 2|\boldsymbol{\xi}|(\mathbf{n} \cdot \mathbf{u})^2, \end{aligned}$$

$$(3.14b) \quad (\boldsymbol{\xi} \cdot \mathbf{v})(\mathbf{n} \cdot \mathbf{v}) \geq (\boldsymbol{\xi} \cdot \mathbf{v}_0)(\mathbf{n} \cdot \mathbf{v}) - 2|\boldsymbol{\xi}|(\mathbf{n} \cdot \mathbf{v})^2.$$

Combining (3.1) and (3.14) yields

$$(3.15) \quad G(\mathbf{n}, \mathbf{u}, \mathbf{v}) \geq G(\mathbf{n}, \mathbf{u}_0, \mathbf{v}_0) - 4\gamma(\mathbf{n})|\boldsymbol{\xi}|((\mathbf{n} \cdot \mathbf{u})^2 + (\mathbf{n} \cdot \mathbf{v})^2).$$

Finally, by (3.2) in lemma 3.1, the estimation of $\gamma^2(\mathbf{u} \times \mathbf{v})$ (3.13), and the estimation of $G(\mathbf{n}, \mathbf{u}, \mathbf{v})$ (3.15), we obtain

$$\begin{aligned} F_K(\mathbf{n}, \mathbf{u}, \mathbf{v}) - \gamma^2(\mathbf{u} \times \mathbf{v}) &\geq \gamma(\mathbf{n})^2(\cos \theta_{2,1})^2 - 2\gamma(\mathbf{n}) \cos \theta_{2,1} ((\boldsymbol{\xi} \cdot \mathbf{v}_0)(\mathbf{n} \cdot \mathbf{u}) + (\boldsymbol{\xi} \cdot \mathbf{u}_0)(\mathbf{n} \cdot \mathbf{v})) \\ &\quad + (\gamma(\mathbf{n})K(\mathbf{n}) - 4|\boldsymbol{\xi}|^2 - 8\gamma(\mathbf{n})|\boldsymbol{\xi}| - 16C_1)((\mathbf{n} \cdot \mathbf{u})^2 + (\mathbf{n} \cdot \mathbf{v})^2) \\ &\geq \gamma(\mathbf{n})^2(\cos \theta_{2,1})^2 - 2\gamma(\mathbf{n})|\cos \theta_{2,1}||\boldsymbol{\xi}|((\mathbf{n} \cdot \mathbf{u}) + (\mathbf{n} \cdot \mathbf{v})) \\ &\quad + 2|\boldsymbol{\xi}|^2((\mathbf{n} \cdot \mathbf{u})^2 + (\mathbf{n} \cdot \mathbf{v})^2) \\ &\geq 0. \end{aligned}$$

Thus we have $F_K(\mathbf{n}, \mathbf{u}, \mathbf{v}) \geq \gamma^2(\mathbf{u} \times \mathbf{v})$ for $\mathbf{n} = (0, 0, 1)^T$. And since the constant $K(\mathbf{n})$ only depends on $\gamma(\mathbf{n})$, the proof is valid for arbitrary $\mathbf{n} \in \mathbb{S}^2$. \square

Theorem 3.3 indicates that the set $\left\{k(\mathbf{n}) \mid F_k(\mathbf{n}, \mathbf{u}, \mathbf{v}) \geq \gamma^2(\mathbf{u} \times \mathbf{v}), \quad \forall \mathbf{u}, \mathbf{v} \in \mathbb{S}^2\right\}$ contains an element $K(\mathbf{n}) < \infty$, and thus is not empty. Together with the fact $k_0(\mathbf{n}) \geq \gamma(\mathbf{n})$ yields the existence of $k_0(\mathbf{n})$.

COROLLARY 3.4 (existence of the minimal stabilizing function). *Suppose $\gamma(\mathbf{n}) \in C^2$ with $\gamma(\mathbf{n}) = \gamma(-\mathbf{n})$. Then the minimal stabilizing function $k_0(\mathbf{n})$ in (2.26) is well-defined.*

Finally, we point out the minimal stabilizing function $k_0(\mathbf{n})$ is determined by $\gamma(\mathbf{n})$. And similar to the 2D result in [5], this map is sub-linear.

THEOREM 3.5 (positive homogeneity and subadditivity). *Suppose $\gamma(\mathbf{n}) = \gamma_1(\mathbf{n}) + \gamma_2(\mathbf{n})$. Let $k_0(\mathbf{n}), k_1(\mathbf{n}), k_2(\mathbf{n})$ be the minimal stabilizing function of $\gamma(\mathbf{n}), \gamma_1(\mathbf{n}), \gamma_2(\mathbf{n})$, respectively, we know that*

- $\forall c > 0$, $ck_0(\mathbf{n})$ is the stabilizing function of $c\gamma(\mathbf{n})$;
- $k_0(\mathbf{n}) \leq k_1(\mathbf{n}) + k_2(\mathbf{n})$.

Proof. The proof of positive homogeneity is similar to the proof of lemma 4.4 in [5], thus we only prove subadditivity. Here we use $\boldsymbol{\xi}, \boldsymbol{\xi}_1, \boldsymbol{\xi}_2$ to denote the $\boldsymbol{\xi}$ vector for $\gamma(\mathbf{n}), \gamma_1(\mathbf{n}), \gamma_2(\mathbf{n})$, respectively.

Since $k_1(\mathbf{n})$ is the minimal stabilizing function of $\gamma_1(\mathbf{n})$. For any $t \in \mathbb{R}$, we have

$$(3.16) \quad \begin{aligned} &\frac{1}{2}\mathbf{u}^T \mathbf{Z}_{k_1}(\mathbf{n})\mathbf{u} + \frac{t^2}{2}\mathbf{v}^T \mathbf{Z}_{k_1}(\mathbf{n})\mathbf{v} - t\gamma_1(\mathbf{u} \times \mathbf{v}) \\ &\geq 2\sqrt{\frac{t^2}{4}F_{k_1}(\mathbf{n}, \mathbf{u}, \mathbf{v}) - t\gamma_1(\mathbf{u} \times \mathbf{v})} \\ &\geq 0. \end{aligned}$$

And this inequality is also true for $\gamma_2(\mathbf{n})$. Add the two inequalities together, and noticing $\boldsymbol{\xi} = \boldsymbol{\xi}_1 + \boldsymbol{\xi}_2$, it yields that

$$(3.17) \quad \frac{1}{2} \mathbf{u}^T \mathbf{Z}_{k_1+k_2}(\mathbf{n}) \mathbf{u} + \frac{t^2}{2} \mathbf{v}^T \mathbf{Z}_{k_1+k_2} \mathbf{v} - t\gamma(\mathbf{u} \times \mathbf{v}) \geq 0, \quad \forall t \in \mathbb{R},$$

which means its discriminant $\gamma^2(\mathbf{u} \times \mathbf{v}) - F_{k_1+k_2}(\mathbf{n}, \mathbf{u}, \mathbf{v}) \leq 0$. And the subadditivity is a direct conclusion from the definition of minimal stabilizing function (2.26). \square

3.2. Proof of the main theorem. By establishing the existence of $k_0(\mathbf{n})$, we now have enough tools to prove (2.27b) in theorem 2.3. To simplify the proof, we first introduce the following alternative definition for the surface gradient operator ∇_S .

LEMMA 3.6. *Suppose σ is a non-degenerated triangle with three vertices $\{\mathbf{q}_1, \mathbf{q}_2, \mathbf{q}_3\}$ ordered counterclockwise. Let f/\mathbf{F} be a scalar-/vector-valued function in $\mathcal{P}^1(\sigma)/[\mathcal{P}^1(\sigma)]^3$, respectively, $\{\mathbf{n}, \boldsymbol{\tau}_1, \boldsymbol{\tau}_2\}$ forms an orthonormal basis. Then the discretized surface gradient operator ∇_S in (2.21) satisfies*

$$(3.18a) \quad \nabla_S f = (\partial_{\boldsymbol{\tau}_1} f) \boldsymbol{\tau}_1 + (\partial_{\boldsymbol{\tau}_2} f) \boldsymbol{\tau}_2,$$

$$(3.18b) \quad \nabla_S \mathbf{F} = (\partial_{\boldsymbol{\tau}_1} \mathbf{F}) \boldsymbol{\tau}_1^T + (\partial_{\boldsymbol{\tau}_2} \mathbf{F}) \boldsymbol{\tau}_2^T,$$

where $\partial_{\boldsymbol{\tau}} f$ denotes the directional derivative of f with respect to $\boldsymbol{\tau}$.

Proof. It suffices to prove (3.18a). Let $\mathbf{x} = \lambda_1 \mathbf{q}_1 + \lambda_2 \mathbf{q}_2 + \lambda_3 \mathbf{q}_3$ with $\lambda_1 + \lambda_2 + \lambda_3 = 1$ be a point in σ . We observe that

$$(3.19) \quad \begin{aligned} (\mathbf{q}_3 - \mathbf{q}_2) \times \mathbf{n} \cdot (\mathbf{x} - \mathbf{q}_3) &= (\mathbf{x} - \mathbf{q}_3) \times (\mathbf{q}_3 - \mathbf{q}_2) \cdot \mathbf{n} \\ &= (-\lambda_1(\mathbf{q}_3 - \mathbf{q}_1) - \lambda_2(\mathbf{q}_3 - \mathbf{q}_2)) \times (\mathbf{q}_3 - \mathbf{q}_2) \cdot \mathbf{n} \\ &= -\lambda_1(\mathbf{q}_2 - \mathbf{q}_1 + \mathbf{q}_3 - \mathbf{q}_2) \times (\mathbf{q}_3 - \mathbf{q}_2) \cdot \mathbf{n} \\ &= -\lambda_1 |\mathcal{J}\{\sigma\}|. \end{aligned}$$

Thus $\lambda_1 = \frac{(\mathbf{q}_2 - \mathbf{q}_3) \times \mathbf{n}}{|\mathcal{J}\{\sigma\}|} \cdot (\mathbf{x} - \mathbf{q}_3)$, and λ_2, λ_3 can be derived similarly.

By definition of the directional derivative, we deduce that.

$$(3.20) \quad \begin{aligned} \partial_{\boldsymbol{\tau}_1} f &= \lim_{h \rightarrow 0} \frac{f(\mathbf{x} + h\boldsymbol{\tau}_1) - f(\mathbf{x})}{h} \\ &= \lim_{h \rightarrow 0} \frac{1}{h} \left(f(\mathbf{q}_1) \frac{(\mathbf{q}_2 - \mathbf{q}_3) \times \mathbf{n}}{|\mathcal{J}\{\sigma\}|} \cdot (h\boldsymbol{\tau}_1) \right. \\ &\quad \left. + f(\mathbf{q}_2) \frac{(\mathbf{q}_3 - \mathbf{q}_1) \times \mathbf{n}}{|\mathcal{J}\{\sigma\}|} \cdot (h\boldsymbol{\tau}_1) + f(\mathbf{q}_3) \frac{(\mathbf{q}_1 - \mathbf{q}_2) \times \mathbf{n}}{|\mathcal{J}\{\sigma\}|} \cdot (h\boldsymbol{\tau}_1) \right) \\ &= \nabla_S f \cdot \boldsymbol{\tau}_1. \end{aligned}$$

Similarly, we have $\partial_{\boldsymbol{\tau}_2} f = \nabla_S f \cdot \boldsymbol{\tau}_2$. Since $\{\mathbf{n}, \boldsymbol{\tau}_1, \boldsymbol{\tau}_2\}$ forms an orthonormal basis, by vector decomposition and $\nabla_S f \cdot \mathbf{n} = 0$, we obtain

$$(3.21) \quad \begin{aligned} \nabla_S f &= (\nabla_S f \cdot \mathbf{n}) \mathbf{n} + (\nabla_S f \cdot \boldsymbol{\tau}_1) \boldsymbol{\tau}_1 + (\nabla_S f \cdot \boldsymbol{\tau}_2) \boldsymbol{\tau}_2 \\ &= (\partial_{\boldsymbol{\tau}_1} f) \boldsymbol{\tau}_1 + (\partial_{\boldsymbol{\tau}_2} f) \boldsymbol{\tau}_2, \end{aligned}$$

which is the desired identity. \square

With the help of (3.18), we can then give the following upperbound for the summand $\gamma(\mathbf{n})|\sigma|$ in the discretized energy W (2.24b).

LEMMA 3.7. Suppose $\sigma, \bar{\sigma}$ are two non-degenerated triangles with counterclockwisely ordered vertices $\{\mathbf{q}_1, \mathbf{q}_2, \mathbf{q}_3\}, \{\bar{\mathbf{q}}_1, \bar{\mathbf{q}}_2, \bar{\mathbf{q}}_3\}$ and outward unit normal vectors $\mathbf{n}, \bar{\mathbf{n}}$, respectively. \mathbf{X} is a vector valued function in $[\mathcal{P}^1(\sigma)]^3$ satisfying $\mathbf{X}(\mathbf{q}_i) = \bar{\mathbf{q}}_i, i = 1, 2, 3$. Then for any $k(\mathbf{n}) \geq k_0(\mathbf{n})$, the following inequality holds

$$(3.22) \quad \frac{1}{6}|\sigma| \sum_{i=1}^3 (\mathbf{Z}_k(\mathbf{n}) \nabla_S \mathbf{X}((\mathbf{q}_i)^-) : \nabla_S \mathbf{X}((\mathbf{q}_i)^-)) \geq \gamma(\bar{\mathbf{n}})|\bar{\sigma}|.$$

Proof. Since $\mathbf{X} \in [\mathcal{P}^1(\sigma)]^3$, its derivative $\nabla_S \mathbf{X}$ is a constant in σ . Suppose $\{\mathbf{n}, \boldsymbol{\tau}_1, \boldsymbol{\tau}_2\}$ forms an orthonormal basis, by applying (3.18b), we obtain

$$(3.23) \quad \nabla_S \mathbf{X}((\mathbf{q}_i)^-) = (\partial_{\boldsymbol{\tau}_1} \mathbf{X}) \boldsymbol{\tau}_1^T + (\partial_{\boldsymbol{\tau}_2} \mathbf{X}) \boldsymbol{\tau}_2^T, \quad i = 1, 2, 3.$$

Let $\partial_{\boldsymbol{\tau}_1} \mathbf{X} = s\mathbf{u}, \partial_{\boldsymbol{\tau}_2} \mathbf{X} = t\mathbf{v}$, where $s, t > 0$ and $\mathbf{u}, \mathbf{v} \in \mathbb{S}^2$. Substituting this and the definition of $\mathbf{Z}_k(\mathbf{n})$ (2.8) into the LHS of (3.22) yields that

$$(3.24) \quad \begin{aligned} & \frac{1}{6}|\sigma| \sum_{i=1}^3 (\mathbf{Z}_k(\mathbf{n}) \nabla_S \mathbf{X}((\mathbf{q}_i)^-) : \nabla_S \mathbf{X}((\mathbf{q}_i)^-)) \\ &= \frac{1}{2}|\sigma| (\mathbf{Z}_k(\mathbf{n})(s\mathbf{u}\boldsymbol{\tau}_1^T + t\mathbf{v}\boldsymbol{\tau}_2^T)) : (s\mathbf{u}\boldsymbol{\tau}_1^T + t\mathbf{v}\boldsymbol{\tau}_2^T) \\ &= \frac{1}{2}|\sigma| (s^2(\boldsymbol{\tau}_1 \cdot \boldsymbol{\tau}_1)\mathbf{u}^T \mathbf{Z}_k(\mathbf{n})\mathbf{u} + t^2(\boldsymbol{\tau}_2 \cdot \boldsymbol{\tau}_2)\mathbf{v}^T \mathbf{Z}_k(\mathbf{n})\mathbf{v}) \\ &\geq |\sigma||st|\sqrt{F_k(\mathbf{n}, \mathbf{u}, \mathbf{v})} \geq |\sigma||st|\gamma(\mathbf{u} \times \mathbf{v}). \end{aligned}$$

For the RHS of (3.22), since $\bar{\sigma} = \mathbf{X}(\sigma)$, it holds that

$$(3.25) \quad \gamma(\bar{\mathbf{n}})|\bar{\sigma}| = \gamma(\bar{\mathbf{n}}) \int_{\sigma} |\partial_{\boldsymbol{\tau}_1} \mathbf{X} \times \partial_{\boldsymbol{\tau}_2} \mathbf{X}| dA = |\sigma||st|\gamma(\bar{\mathbf{n}})|\mathbf{u} \times \mathbf{v}|.$$

Finally, since $\mathbf{X} \in [\mathcal{P}^1(\sigma)]^3$, for \mathbf{p} and $\mathbf{p} + h\boldsymbol{\tau}_1$ in σ , we have $\mathbf{X}(\mathbf{p} + h\boldsymbol{\tau}_1)$ and $\mathbf{X}(\mathbf{p})$ in $\bar{\sigma}$. From the definition of directional derivative for function in $[\mathcal{P}^1(\sigma)]^3$, we get

$$(3.26) \quad s\mathbf{u} \cdot \bar{\mathbf{n}} = (\partial_{\boldsymbol{\tau}_1} \mathbf{X}) \cdot \bar{\mathbf{n}} = \frac{\mathbf{X}(\mathbf{p} + h\boldsymbol{\tau}_1) - \mathbf{X}(\mathbf{p})}{h} \cdot \bar{\mathbf{n}} = 0,$$

and similarly $\mathbf{v} \cdot \bar{\mathbf{n}} = 0$, thus $\gamma(\mathbf{u} \times \mathbf{v}) = |\mathbf{u} \times \mathbf{v}|\gamma(\bar{\mathbf{n}})$. This equation together with (3.24) and (3.25) yield the desired inequality (3.22). \square

With the help of lemma (3.7), we can then prove the energy stability part (2.27b) in our main theorem 2.3.

Proof. First for any $\mathbf{p} \in \mathbb{S}^2$, since $k(\mathbf{n}) \geq k_0(\mathbf{n})$, we have

$$(3.27) \quad \mathbf{p}^T \mathbf{Z}_k(\mathbf{n}) \mathbf{p} = \gamma(\mathbf{n}) - 2(\boldsymbol{\xi} \cdot \mathbf{p})(\mathbf{n} \cdot \mathbf{p}) + k(\mathbf{n})(\mathbf{n} \cdot \mathbf{p})^2 \geq 0,$$

thus $\mathbf{Z}_k(\mathbf{n})$ is positive definite. By Cauchy inequality, it holds that

$$(3.28) \quad \begin{aligned} & \langle \mathbf{Z}_k(\mathbf{n}^m) \nabla_S \mathbf{X}^{m+1}, \nabla_S (\mathbf{X}^{m+1} - \mathbf{X}^m) \rangle_{S^m} \\ &\geq \frac{1}{2} \langle \mathbf{Z}_k(\mathbf{n}^m) \nabla_S \mathbf{X}^{m+1}, \nabla_S \mathbf{X}^{m+1} \rangle_{S^m} - \frac{1}{2} \langle \mathbf{Z}_k(\mathbf{n}^m) \nabla_S \mathbf{X}^m, \nabla_S \mathbf{X}^m \rangle_{S^m}. \end{aligned}$$

Suppose $\{\mathbf{n}_j^m, \boldsymbol{\tau}_{j,1}^m, \boldsymbol{\tau}_{j,2}^m\}$ forms an orthonormal basis for $1 \leq j \leq J$, by (3.18b) we obtain

$$\begin{aligned}
& \frac{1}{2} \langle \mathbf{Z}_k(\mathbf{n}^m) \nabla_S \mathbf{X}^m, \nabla_S \mathbf{X}^m \rangle_{S^m} \\
&= \frac{1}{6} \sum_{j=1}^J \sum_{i=1}^3 |\sigma_j^m| (\mathbf{Z}_k(\mathbf{n}_j^m) \nabla_S \mathbf{X}^m|_{\sigma_j^m((\mathbf{q}_{j,i}^m)^-)} : \nabla_S \mathbf{X}^m|_{\sigma_j^m((\mathbf{q}_{j,i}^m)^-)} \\
&= \frac{1}{2} \sum_{j=1}^J |\sigma_j^m| (\boldsymbol{\tau}_{j,1}^m \cdot \mathbf{Z}_k(\mathbf{n}_j^m) \boldsymbol{\tau}_{j,1}^m + \boldsymbol{\tau}_{j,2}^m \cdot \mathbf{Z}_k(\mathbf{n}_j^m) \boldsymbol{\tau}_{j,2}^m) \\
&= \frac{1}{2} \sum_{j=1}^J |\sigma_j^m| \gamma(\mathbf{n}_j^m) (\boldsymbol{\tau}_{j,1}^m \cdot \boldsymbol{\tau}_{j,1}^m + \boldsymbol{\tau}_{j,2}^m \cdot \boldsymbol{\tau}_{j,2}^m) \\
(3.29) \quad &= \sum_{j=1}^J |\sigma_j^m| \gamma(\mathbf{n}_j^m) = W^m.
\end{aligned}$$

Then apply lemma (3.7) for $\sigma = \sigma_j^m, \bar{\sigma} = \sigma_j^{m+1}$ and $\mathbf{X} = \mathbf{X}^{m+1}|_{\sigma_j^m}$, we know that

$$(3.30) \quad \frac{1}{6} |\sigma_j^m| \sum_{i=1}^3 (\mathbf{Z}_k(\mathbf{n}_j^m) \nabla_S \mathbf{X}|_{\sigma_j^m((\mathbf{q}_i)^-)} : \nabla_S \mathbf{X}|_{\sigma_j^m((\mathbf{q}_i)^-)} \geq \gamma(\mathbf{n}_j^{m+1}) |\sigma_j^{m+1}|.$$

And this inequality holds for all $1 \leq j \leq J$. Summing (3.30) for $j = 1, 2, \dots, J$ and combining (3.28) and (3.29) yields that

$$(3.31) \quad \langle \mathbf{Z}_k(\mathbf{n}^m) \nabla_S \mathbf{X}^{m+1}, \nabla_S (\mathbf{X}^{m+1} - \mathbf{X}^m) \rangle_{S^m} \geq W^{m+1} - W^m.$$

Finally, choosing $\psi = \mu^{m+1}$ in (2.22a) and $\boldsymbol{\omega} = \mathbf{X}^{m+1}$ in (2.22b), together with (3.31) yields that

$$(3.32) \quad W^{m+1} - W^m \leq \tau (\nabla_S \mu^{m+1}, \nabla_S \mu^{m+1})_{S^m} \leq 0.$$

Since this inequality is valid for all m , the unconditionally energy stable part (2.27b) in theorem 2.3 is proved. \square

4. Numerical results. In this section, we first state the setup for solving the SP-PFEM (2.22). Then we present several numerical computations, including the convergence test and the structural preserving test. Finally, we apply (2.22) to simulate the surface evolution for different anisotropic energies.

The minimal stabilizing function $k_0(\mathbf{n})$ is given by the bilinear interpolation, where the interpolation points are $\mathbf{n}_{i,j} = (\cos \phi_i \cos \theta_j, \cos \phi_i \sin \theta_j, \sin \phi_i)^T$, $\phi_i = -\frac{\pi}{2} + \frac{i}{10}\pi$, $\theta_j = -\pi + \frac{j}{5}\pi$, $0 \leq i, j \leq 10$, and the $k_0(\mathbf{n}_{i,j})$ is given by solving (2.26). The surface energy matrix $\mathbf{Z}_k(\mathbf{n})$ as well as the SP-PFEM (2.22) is thus determined by giving a stabilizing function $k(\mathbf{n}) \geq k_0(\mathbf{n})$.

The fully-implicit linear system (2.22) is solved by using the Newton's iterative method provided in [8]. And for each discrete time level $t_m = m\tau$, the iteration is terminated when $\|\mathbf{X}^\delta\|_\infty \leq 10^{-12}$, $\|\mu^\delta\| \leq 10^{-12}$, where $(\mathbf{X}^\delta(\cdot), \mu^\delta(\cdot)) \in [\mathbb{K}^m]^3 \times \mathbb{K}^m$ is the Newton direction.

Given an initial shape S_0 , we generate its approximation $S^0 = \cup_{j=1}^J \bar{\sigma}_j^0$ with J triangles $\{\sigma_j^0\}_{j=1}^J$ and I vertices $\{\mathbf{q}_i^0\}_{i=1}^I$ by using a matlab toolbox called *CFDTool*

[36] with a given parameter mesh size h . For the time step size τ and the mesh size h , we denote the solution of (2.22) with the initial approximation S_h^0 with $J(h)$ triangles and $I(h)$ vertices at t_m by $(\mathbf{X}_{h,\tau}^m, \mu_{h,\tau}^m)$. And we define $\mathbf{X}_{h,\tau}(t)$ by

$$(4.1) \quad \mathbf{X}_{h,\tau}(t) = \frac{t - t_m}{\tau} \mathbf{X}_{h,\tau}^m + \frac{t_{m+1} - t}{\tau} \mathbf{X}_{h,\tau}^{m+1}, \quad \forall t \in [t_m, t_{m+1}), m \geq 0.$$

And $S_{h,\tau}(t)$ is defined similarly.

To test the convergence rate of (2.22), we adopt the manifold distance $M(\cdot, \cdot)$ to measure the difference between two closed surfaces S_1 and S_2 , which is given by

$$(4.2) \quad M(S_1, S_2) := 2|\Omega_1 \cup \Omega_2| - |\Omega_1| - |\Omega_2|,$$

where we denote Ω_1 and Ω_2 to be the interior of S_1 and S_2 , respectively. Based on the manifold distance, the numerical error is defined as

$$(4.3) \quad e_{h,\tau}(t) := M(S_{h,\tau}(t), S(t)).$$

Here $S(t)$ is approximated by the refined mesh $S_{h_e, \tau_e}(t)$ with $k(\mathbf{n}) = k_0(\mathbf{n})$, where $h_e = 2^{-4}$ and $\tau_e = \frac{2}{25}h_e^2$.

In the numerical experiments for convergence rates, the time step size and the mesh size are chosen as $\tau = \frac{2}{25}h^2$, the initial shape S_0 is chosen as a $2 \times 2 \times 1$ cuboid, and its approximation is a polyhedron S_{h_e, τ_e}^0 with 10718 triangles and 5361 vertices. We consider the following five cases of the anisotropic surface energy $\gamma(\mathbf{n})$ as well as the stabilizing function $k(\mathbf{n})$:

- Case 1: $\gamma(\mathbf{n}) = 1 + \frac{1}{4}(n_1^4 + n_2^4 + n_3^4)$, $k(\mathbf{n}) = k_0(\mathbf{n})$;
- Case 2: $\gamma(\mathbf{n}) = 1 + \frac{1}{2}(n_1^4 + n_2^4 + n_3^4)$, $k(\mathbf{n}) = k_0(\mathbf{n})$;
- Case 3: $\gamma(\mathbf{n}) = (n_1^4 + n_2^4 + n_3^4)^{\frac{1}{4}}$, $k(\mathbf{n}) = k_0(\mathbf{n})$;
- Case 4: $\gamma(\mathbf{n}) = (n_1^4 + n_2^4 + n_3^4)^{\frac{1}{4}}$, $k(\mathbf{n}) = k_0(\mathbf{n}) + 1$;
- Case 5: $\gamma(\mathbf{n}) = (n_1^4 + n_2^4 + n_3^4)^{\frac{1}{4}}$, $k(\mathbf{n}) = k_0(\mathbf{n}) + 2$;
- Case 6: $\gamma(\mathbf{n}) = (n_1^4 + n_2^4 + n_3^4)^{\frac{1}{4}}$, $k(\mathbf{n}) = k_0(\mathbf{n}) + 5$.

The numerical errors are listed in TABLE 4. We note that while the $\gamma(\mathbf{n})$ and $k(\mathbf{n})$ are different in each cases, the convergence rates for this manifold error are all about second order in h . This result indicates the proposed SP-PFEM (2.22) has a good robustness in convergence rate, and we can choose large $k(\mathbf{n})$ such as $k(\mathbf{n}) \equiv \sup_{\mathbf{n} \in \mathbb{S}^2} k_0(\mathbf{n})$ to avoid the computation cost in bilinear interpolation without loss of efficiency.

To examine the volume conservation and unconditionally energy dissipation, we consider these two indicators, the normalized volume change $\frac{\Delta V(t)}{V(0)} := \frac{V(t) - V(0)}{V(0)}$ and the normalized energy $\frac{W(t)}{W(0)}$; and we choose the initial shape to be a $2 \times 2 \times 1$ ellipsoid. Figure 4.1 shows the normalized volume change $\frac{\Delta V(t)}{V(0)}$ for the anisotropy in Case 1, Case 2, Case 3, with fixed $h = 2^{-3}$, $\tau = \frac{2}{25}h^2$ in (a), (b), (c), respectively. We find the order of magnitude of the volume change $\Delta V(t)$ is 10^{-15} , which is close to the machine epsilon 10^{-16} , and thus indicates the volume is well conserved. Figure 4.2 plot the normalized energy $\frac{W(t)}{W(0)}$ for different cases and mesh size h with $\tau = \frac{2}{25}h^2$ and for different τ with a constant mesh size $h = 2^{-4}$, respectively. We observe the normalized energy $\frac{W(t)}{W(0)}$ is monotonically decreasing in time, even for the relatively large time step size $\tau = 0.01$. And these graphs also suggest the stabilizing function $k(\mathbf{n})$ does not infect the energy, and we can choose a relatively large stabilizing function $k(\mathbf{n})$, which

(h, τ)	$e_{h,\tau}(\frac{1}{2})$ Case 1	order	$e_{h,\tau}(\frac{1}{2})$ Case 2	order	$e_{h,\tau}(\frac{1}{2})$ Case 3	order
(h_0, τ_0)	1.24E-1	-	1.47E-1	-	1.12E-1	-
$(\frac{h_0}{2}, \frac{\tau_0}{4})$	3.06E-2	2.01	3.54E-2	2.05	2.82E-2	1.98
$(\frac{h_0}{2^2}, \frac{\tau_0}{4^2})$	7.90E-3	1.96	8.74E-3	2.02	7.54E-3	1.90
(h, τ)	$e_{h,\tau}(\frac{1}{2})$ Case 4	order	$e_{h,\tau}(\frac{1}{2})$ Case 5	order	$e_{h,\tau}(\frac{1}{2})$ Case 6	order
(h_0, τ_0)	1.10E-1	-	1.12E-1	-	1.12E-1	-
$(\frac{h_0}{2}, \frac{\tau_0}{4})$	2.83E-2	1.96	2.89E-2	1.96	3.09E-2	1.99
$(\frac{h_0}{2^2}, \frac{\tau_0}{4^2})$	7.48E-3	1.92	7.58E-3	1.93	7.86E-3	1.97

(h, τ)	$e_{h,\tau}(1)$ Case 1	order	$e_{h,\tau}(1)$ Case 2	order	$e_{h,\tau}(1)$ Case 3	order
(h_0, τ_0)	1.46E-1	-	1.22E-1	-	1.11E-1	-
$(\frac{h_0}{2}, \frac{\tau_0}{4})$	3.52E-2	2.05	3.01E-2	2.02	2.74E-2	2.02
$(\frac{h_0}{2^2}, \frac{\tau_0}{4^2})$	8.67E-3	2.02	7.75E-3	1.96	7.21E-3	1.93
(h, τ)	$e_{h,\tau}(1)$ Case 4	order	$e_{h,\tau}(1)$ Case 5	order	$e_{h,\tau}(1)$ Case 6	order
(h_0, τ_0)	1.10E-1	-	1.10E-1	-	1.13E-1	-
$(\frac{h_0}{2}, \frac{\tau_0}{4})$	2.76E-2	1.99	2.80E-2	1.97	2.90E-2	1.96
$(\frac{h_0}{2^2}, \frac{\tau_0}{4^2})$	7.23E-3	1.93	7.36E-3	1.93	7.56E-3	1.94

TABLE 4.1

Numerical error $e_{h,\tau}$ at time $T = \frac{1}{2}, 1$ and the convergence rate for simulating the anisotropic surface diffusion start from a $2 \times 2 \times 1$ cuboid with different anisotropic energies $\gamma(\mathbf{n})$ and stabilizing functions $k(\mathbf{n})$ given in Case 1-6. The mesh size, time step size, number of triangles and number of vertices for the coarse shapes are $(h_0 := 2^{-1}, \tau_0 := \frac{2^{-1}}{25}, 140, 72)$, and then $(2^{-2}, \frac{2^{-3}}{25}, 624, 314)$, $(2^{-3}, \frac{2^{-5}}{25}, 2502, 1253)$.

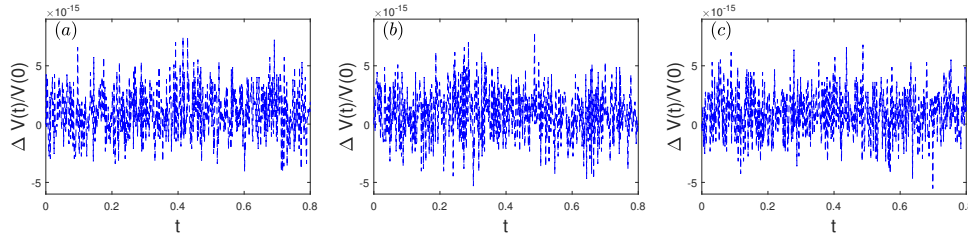


FIG. 4.1. Plot of the normalized volume change $\frac{\Delta V(t)}{V(0)}$ for different anisotropic energies in Case 1 (a), Case 2 (b) and Case 3 (c).

consists the result in convergence rate test. And the above volume and energy tests validate the theorem (2.3) numerically.

Finally, we use (2.22) to investigate the motion by anisotropic surface diffusion with different anisotropies. We consider the weak anisotropy $\gamma(\mathbf{n}) = \sqrt{n_1^2 + n_2^2 + 2n_3^2}$ with $k(\mathbf{n}) = k_0(\mathbf{n})$ first. The evolutions of a smooth $2 \times 2 \times 1$ ellipsoid and a non-smooth $2 \times 2 \times 1$ cuboid are shown in figure 4.3 and figure 4.4, respectively. We choose the mesh size $h = 2^{-4}$ and the time step size $\tau = \frac{2}{25}h^2$, and the ellipsoid and the cuboid are initially approximated by $K(h) = 10718, I(h) = 5361$ and $K(h) = 32768, I(h) = 16386$, respectively. By comparing the two figures, we find the two numerical equilibriums are close in shape, which indicates our scheme (2.22) is stable in catching the equilibrium shape for different initial shapes. We can see that the

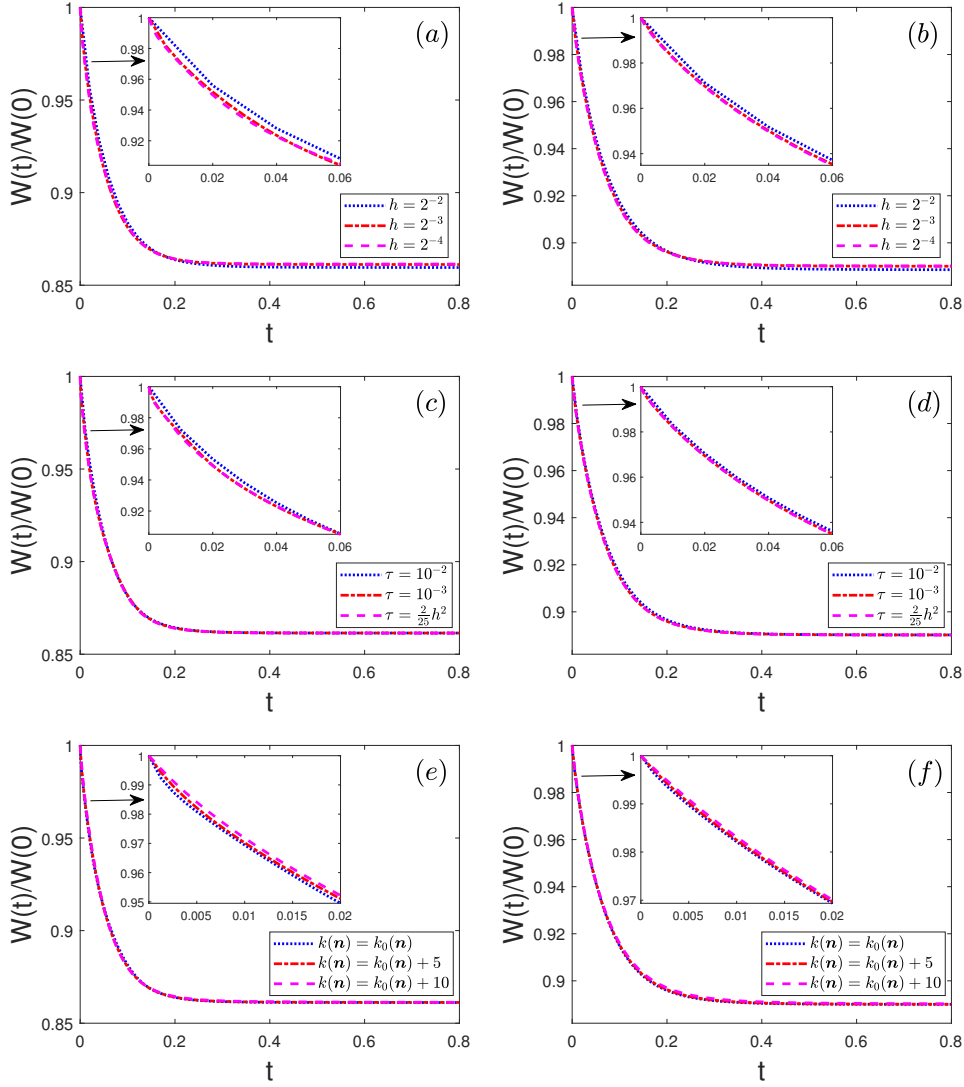


FIG. 4.2. Plot of the normalized energy $\frac{W(t)}{W(0)}$ for weak/strong anisotropy $\gamma(\mathbf{n}) = 1 + \frac{1}{4}(n_1^4 + n_2^4 + n_3^4)$ or $\gamma(\mathbf{n}) = 1 + \frac{1}{2}(n_1^4 + n_2^4 + n_3^4)$ for $k(\mathbf{n}) = k_0(\mathbf{n})$ with different h and τ (a), (b); for fixed $h = 2^{-4}$ with different τ (c), (d); for $h = 2^{-4}, \tau = \frac{2}{25}h^2$ with different $k(\mathbf{n})$ (e), (f), respectively.

meshes are well distributed during the evolution, and we do not need to remesh the surface.

Then we show the evolution of a strong anisotropy $\gamma(\mathbf{n}) = 1 + \frac{1}{2}(n_1^4 + n_2^4 + n_3^4)$ from a $2 \times 2 \times 1$ cuboid, and the parameters are chosen the same as in previous weak anisotropy. As can be seen from figure 4.5, the large and flat facets may be broken into small facets, and the small facets may also merge into a large facet. Moreover, we note from figure 4.5 that the triangulations become dense at the edges where the facets merge but become sparse at the other edges and at the interior of the facets where the weighted mean curvature μ is almost a constant.

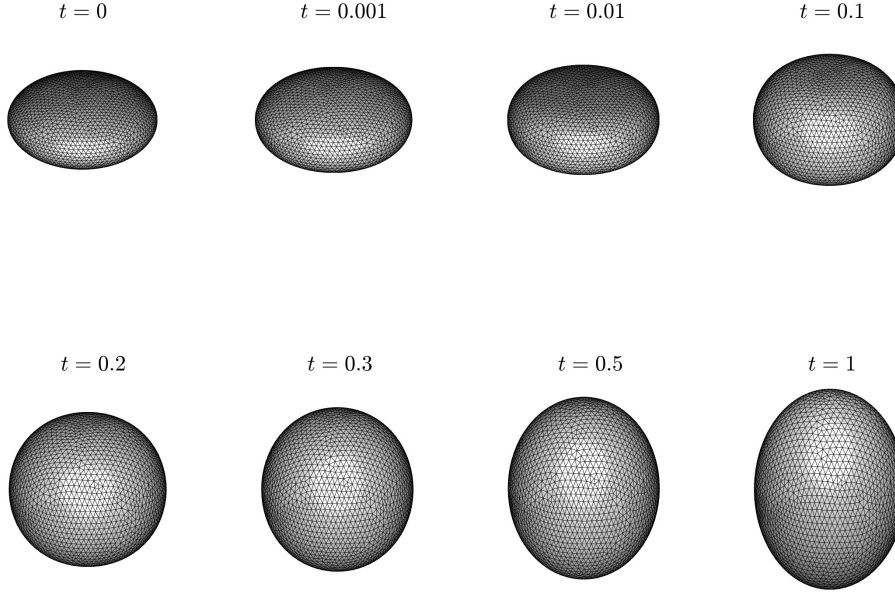


FIG. 4.3. *Evolution of a $2 \times 2 \times 1$ ellipsoid by anisotropic surface diffusion with a weak anisotropy $\gamma(\mathbf{n}) = \sqrt{n_1^2 + n_2^2 + 2n_3^2}$ and $k(\mathbf{n}) = k_0(\mathbf{n})$ at different times.*

5. Conclusions. By generalizing the symmetrized surface energy matrix $Z_k(\mathbf{n})$ into 3D, we proposed a new weak formulation for the weighted mean curvature μ and derived a symmetrized variational formulation. Based on this new variational formulation, we proposed a structural-preserving finite element method (SP-PFEM) for anisotropic surface diffusion in 3D and established its unconditional energy stability for C^2 anisotropies with $\gamma(-\mathbf{n}) = \gamma(\mathbf{n})$ (1.5). Moreover, we constructed the upper bound for the minimal stabilizing function $k_0(\mathbf{n})$, which also gave a promising approach to determine the symmetrized surface energy matrix $Z_k(\mathbf{n})$. Unlike other structural-preserving schemes for anisotropic surface diffusion, our SP-PFEM can work for an arbitrary initial shape and a much broader functional class, the symmetric C^2 functions.

Similar to other PFEMs, our SP-PFEM for 3D anisotropic surface diffusion illustrated a second-order convergence rate, which was also verified by various numerical experiments. We examined the volume is conserved in machine epsilon, and the energy is dissipative, regardless of the choice of the anisotropy $\gamma(\mathbf{n})$, the stabilizing function $k(\mathbf{n})$ and the time step size τ , which matched the prediction of the main theorem 2.3 well. We presented the evolution of both smooth and non-smooth initial shapes with weakly/strongly anisotropic energies. Many interesting phenomena were shown, such as numerical equilibrium, facet breaking, and facet merging.

Finally, We point out that the symmetrized variational formulation (2.14) can be applied to other geometric flows with symmetric anisotropic surface energy, such as the

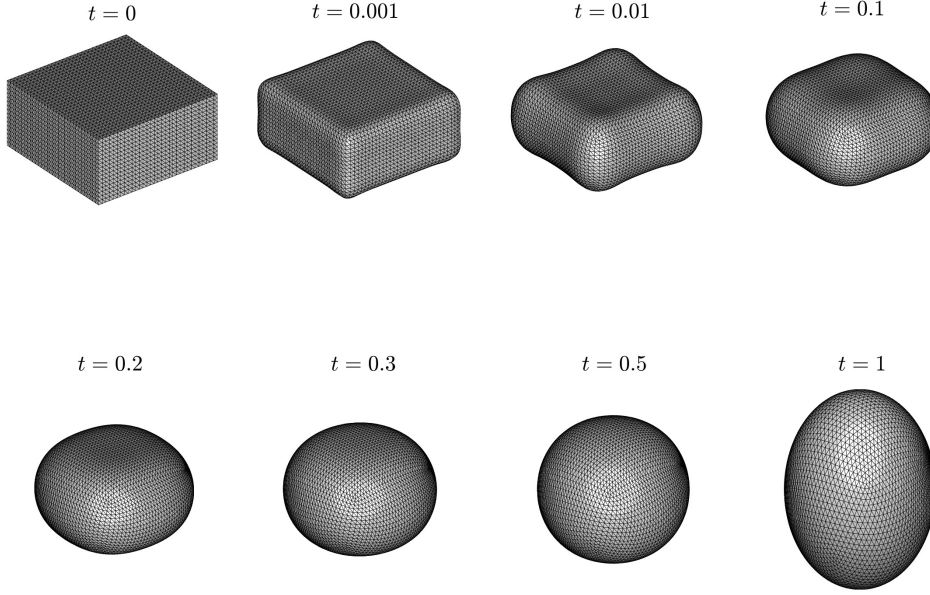


FIG. 4.4. *Evolution of a $2 \times 2 \times 1$ cuboid by anisotropic surface diffusion with a weak anisotropy $\gamma(\mathbf{n}) = \sqrt{n_1^2 + n_2^2 + 2n_3^2}$ and $k(\mathbf{n}) = k_0(\mathbf{n})$ at different times.*

anisotropic mean curvature flow [10], the Stefan problem [13], and the anisotropic elastic flow [15]. Our future work will consider the SP-PFEM for asymmetric anisotropic energies for the 2D and 3D anisotropic surface diffusion.

Appendix A. Remark for several common used anisotropic surface energies

For the ellipsoidal anisotropic surface energy [10]

$$(A.1) \quad \gamma(\mathbf{n}) = \sqrt{\mathbf{n}^T \mathbf{G} \mathbf{n}},$$

where \mathbf{G} is positive definite, we have

$$(A.2) \quad \gamma(\mathbf{p}) = \sqrt{\mathbf{p}^T \mathbf{G} \mathbf{p}}, \quad \forall \mathbf{p} \in \mathbb{R}_*^3 := \mathbb{R}^3 \setminus \{\mathbf{0}\},$$

$$(A.3) \quad \boldsymbol{\xi} = \boldsymbol{\xi}(\mathbf{n}) = \gamma(\mathbf{n})^{-1} \mathbf{G} \mathbf{n}, \quad \forall \mathbf{n} \in \mathbb{S}^1,$$

$$(A.4) \quad \mathbf{H}_\gamma(\mathbf{n}) = \gamma(\mathbf{n})^{-3/2} (\gamma(\mathbf{n})^2 \mathbf{G} - (\mathbf{G} \mathbf{n})(\mathbf{G} \mathbf{n})^T).$$

And we know $\mathbf{H}_\gamma(\mathbf{n})$ is semi-positive definite by Cauchy inequality, which indicates the ellipsoidal anisotropy is weakly anisotropic.

For the l^r -norm ($r \geq 2$) metric anisotropic surface energy [5]

$$(A.5) \quad \gamma(\mathbf{n}) = (|n_1|^r + |n_2|^r + |n_3|^r)^{1/r},$$

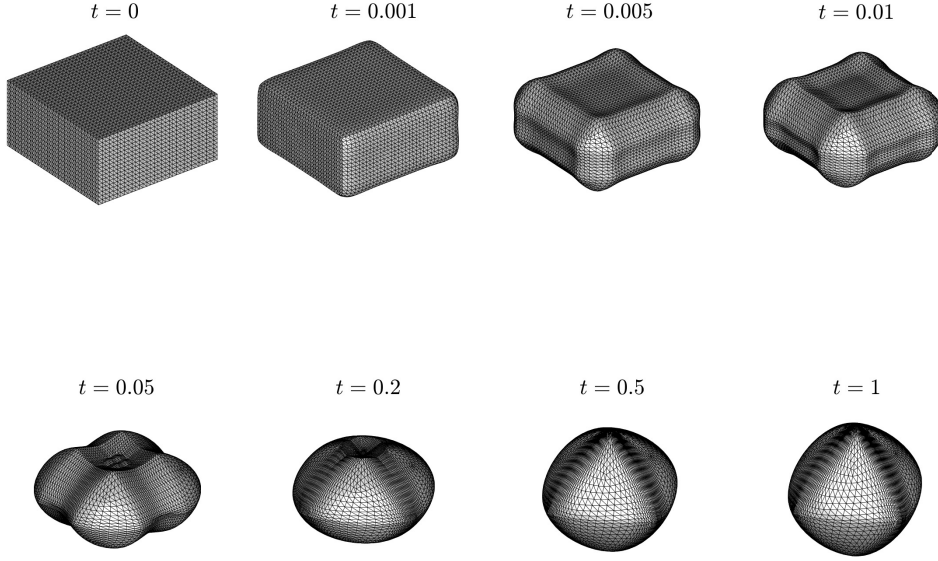


FIG. 4.5. *Evolution of a $2 \times 2 \times 1$ cuboid by anisotropic surface diffusion with a strong anisotropy $\gamma(\mathbf{n}) = 1 + \frac{1}{2}(n_1^4 + n_2^4 + n_3^4)$ and $k(\mathbf{n}) = k_0(\mathbf{n})$ at different times.*

we have

$$(A.6) \quad \gamma(\mathbf{p}) = \|\mathbf{p}\|_{l^r} = (|p_1|^r + |p_2|^r + |p_3|^r)^{\frac{1}{r}}, \quad \forall \mathbf{p} \in \mathbb{R}_*^3,$$

$$(A.7) \quad \boldsymbol{\xi} = \boldsymbol{\xi}(\mathbf{n}) = \gamma(\mathbf{n})^{1-r} \begin{pmatrix} |n_1|^{r-2} n_1 \\ |n_2|^{r-2} n_2 \\ |n_3|^{r-2} n_3 \end{pmatrix}, \quad \forall \mathbf{n} \in \mathbb{S}^1,$$

$$(A.8) \quad \mathbf{H}_\gamma(\mathbf{n}) = (r-1)\gamma(\mathbf{n})^{1-2r} \begin{pmatrix} |n_1|^{r-2}(|n_2|^r + |n_3|^r) & * & * \\ -|n_1 n_2|^{r-2} n_1 n_2 & * & * \\ -|n_1 n_3|^{r-2} n_1 n_3 & * & * \end{pmatrix}.$$

Where the $*$ entries can be deduced from other entries. By checking leading principal minors, we know that $\mathbf{H}_\gamma(\mathbf{n})$ is semi-positive definite. Thus the l^r -norm anisotropy is weakly anisotropic.

For the 4-fold anisotropic surface energy [21]

$$(A.9) \quad \gamma(\mathbf{n}) = 1 + \beta(n_1^4 + n_2^4 + n_3^4),$$

we have

$$(A.10) \quad \gamma(\mathbf{p}) = (p_1^2 + p_2^2 + p_3^2)^{\frac{1}{2}} + \beta(p_1^4 + p_2^4 + p_3^4) (p_1^2 + p_2^2 + p_3^2)^{-\frac{3}{2}},$$

$$(A.11) \quad \boldsymbol{\xi} = \boldsymbol{\xi}(\mathbf{n}) = \mathbf{n} + \beta(4n_1^3 - 3n_1(n_1^4 + n_2^4 + n_3^4), *, *)^T,$$

$$(A.12) \quad \lambda_1(\mathbf{n}) + \lambda_2(\mathbf{n}) = 2(1 - 3\beta) + 36\beta(n_1^2 n_2^2 + n_2^2 n_3^2 + n_3^2 n_1^2).$$

Thus $\gamma(\mathbf{n})$ is strongly anisotropic if $\beta > 1/3$. For $\beta = 1/3$, we know $\lambda_1(\mathbf{n}) + \lambda_2(\mathbf{n}) \geq 0$ and

$$(A.13) \quad \lambda_1(\mathbf{n})\lambda_2(\mathbf{n}) = 4(5(n_1^4 n_2^4 + n_2^4 n_3^4 + n_3^4 n_1^4) + 18n_1^2 n_2^2 n_3^2) \geq 0,$$

which means $\gamma(\mathbf{n})$ is weakly anisotropic. When $\beta = 0$, $\gamma(\mathbf{n})$ collapse to the l^2 -norm, and we have already known such $\gamma(\mathbf{n})$ is weakly anisotropic. We know that $\gamma(\mathbf{n})$ is weakly anisotropic for $0 \leq \beta \leq \frac{1}{3}$ and is strongly anisotropic for $\beta > \frac{1}{3}$.

Finally, for the regularized BGN anisotropic surface energy [12]

$$(A.14) \quad \gamma(\mathbf{n}) = \left(\sum_{l=1}^L (\mathbf{n}^T \mathbf{G}_l \mathbf{n})^{r/2} \right)^{1/r},$$

where $\mathbf{G}_1, \mathbf{G}_2, \dots, \mathbf{G}_L$ are positive definite matrices, we get

$$(A.15) \quad \gamma(\mathbf{p}) = \left(\sum_{l=1}^L (\mathbf{p}^T \mathbf{G}_l \mathbf{p})^{r/2} \right)^{1/r}, \quad \forall \mathbf{p} \in \mathbb{R}_*^3,$$

$$(A.16) \quad \boldsymbol{\xi} = \boldsymbol{\xi}(\mathbf{n}) = \gamma(\mathbf{n})^{1-r} \sum_{l=1}^L \gamma_l^{r-2}(\mathbf{n}) \mathbf{G}_l \mathbf{n} \quad \forall \mathbf{n} \in \mathbb{S}^1,$$

$$(A.17) \quad \mathbf{H}_\gamma(\mathbf{n}) = \gamma(\mathbf{n})^{1-2r} (\mathbf{M}_1 + (r-1)\mathbf{M}_2).$$

where $\gamma_l(\mathbf{n}) := \sqrt{\mathbf{n}^T \mathbf{G}_l \mathbf{n}}$, $l = 1, 2, \dots, L$, and

$$(A.18) \quad \mathbf{M}_1 = \gamma(\mathbf{n})^r \sum_{l=1}^L \gamma_l(\mathbf{n})^{r-4} (\gamma_l(\mathbf{n})^2 \mathbf{G}_l - (\mathbf{G}_l \mathbf{n})(\mathbf{G}_l \mathbf{n})^T),$$

$$(A.19) \quad \mathbf{M}_2 = \gamma(\mathbf{n})^r \sum_{l=1}^L (\mathbf{G}_l \mathbf{n})(\mathbf{G}_l \mathbf{n})^T \gamma_l^{r-4}(\mathbf{n}) - \left(\sum_{l=1}^L \gamma_l^{r-2}(\mathbf{n}) \mathbf{G}_l \mathbf{n} \right) \left(\sum_{l=1}^L \gamma_l^{r-2}(\mathbf{n}) \mathbf{G}_l \mathbf{n} \right)^T.$$

By Cauchy inequality, we obtain that $\mathbf{M}_1, \mathbf{M}_2$ are semi-positive definite. Thus the BGN anisotropy is weakly anisotropic for $r \geq 1$.

REFERENCES

- [1] L. ARMELAO, D. BARRECA, G. BOTTARO, A. GASPAROTTO, S. GROSS, C. MARAGNO, AND E. TONDELLO, *Recent trends on nanocomposites based on cu, ag and au clusters: A closer look*, Coordination Chemistry Reviews, 250 (2006), pp. 1294–1314.
- [2] R. ASARO AND W. TILLER, *Interface morphology development during stress corrosion cracking: Part i. via surface diffusion*, Metallurgical and Materials Transactions B, 3 (1972), pp. 1789–1796.
- [3] E. BÄNSCH, P. MORIN, AND R. H. NOCHETTO, *Surface diffusion of graphs: variational formulation, error analysis, and simulation*, SIAM J. Numer. Anal., 42 (2004), pp. 773–799.
- [4] W. BAO, H. GÄRCKE, R. NÜRNBERG, AND Q. ZHAO, *Volume-preserving parametric finite element methods for axisymmetric geometric evolution equations*, Journal of Computational Physics, 460 (2022), p. 111180.
- [5] W. BAO, W. JIANG, AND Y. LI, *A symmetrized parametric finite element method for anisotropic surface diffusion of closed curves via a cahn-hoffman ξ -vector formulation*, arXiv preprint arXiv:2112.00508, (2021).
- [6] W. BAO, W. JIANG, Y. WANG, AND Q. ZHAO, *A parametric finite element method for solid-state dewetting problems with anisotropic surface energies*, J. Comput. Phys., 330 (2017), pp. 380–400.

- [7] W. BAO AND Q. ZHAO, *A structure-preserving parametric finite element method for surface diffusion*, SIAM Journal on Numerical Analysis, 59 (2021), pp. 2775–2799.
- [8] W. BAO AND Q. ZHAO, *A structure-preserving parametric finite element method for surface diffusion*, SIAM J. Numer. Anal., 59 (2021), pp. 2775–2799.
- [9] J. W. BARRETT, H. GARCKE, AND R. NÜRNBERG, *A parametric finite element method for fourth order geometric evolution equations*, J. Comput. Phys., 222 (2007), pp. 441–467.
- [10] J. W. BARRETT, H. GARCKE, AND R. NÜRNBERG, *Numerical approximation of anisotropic geometric evolution equations in the plane*, IMA J. Numer. Anal., 28 (2008), pp. 292–330.
- [11] J. W. BARRETT, H. GARCKE, AND R. NÜRNBERG, *On the parametric finite element approximation of evolving hypersurfaces in \mathbb{R}^3* , Journal of Computational Physics, 227 (2008), pp. 4281–4307.
- [12] J. W. BARRETT, H. GARCKE, AND R. NÜRNBERG, *A variational formulation of anisotropic geometric evolution equations in higher dimensions*, Numerische Mathematik, 109 (2008), pp. 1–44.
- [13] J. W. BARRETT, H. GARCKE, AND R. NÜRNBERG, *On stable parametric finite element methods for the stefan problem and the mullins–sekerka problem with applications to dendritic growth*, Journal of Computational Physics, 229 (2010), pp. 6270–6299.
- [14] J. W. BARRETT, H. GARCKE, AND R. NÜRNBERG, *Numerical computations of faceted pattern formation in snow crystal growth*, Physical Review E, 86 (2012), p. 011604.
- [15] J. W. BARRETT, H. GARCKE, AND R. NÜRNBERG, *Parametric approximation of isotropic and anisotropic elastic flow for closed and open curves*, Numerische Mathematik, 120 (2012), pp. 489–542.
- [16] O. BEKHTEREVA, Y. GAVRILYUK, V. LIFSHITS, AND B. CHURUSOV, *Indium surface phase formation on si (111) surface and their role in diffusion and desorption. poverkhnost'*, Physika, Khimiia i Mekhanika, 8 (1988), p. 54.
- [17] J. CAHN AND D. HOFFMAN, *A vector thermodynamics for anisotropic surfaces: I. curved and faceted surfaces*, The Selected Works of John W. Cahn, (1998), pp. 315–324.
- [18] J. W. CAHN AND J. E. TAYLOR, *Overview no. 113 surface motion by surface diffusion*, Acta Metall. Mater., 42 (1994), pp. 1045–1063.
- [19] L.-S. CHANG, E. RABKIN, B. STRAUMAL, B. BARETZKY, AND W. GUST, *Thermodynamic aspects of the grain boundary segregation in cu (bi) alloys*, Acta Materialia, 47 (1999), pp. 4041–4046.
- [20] U. CLARENZ, U. DIEWALD, AND M. RUMPF, *Anisotropic geometric diffusion in surface processing*, IEEE Visualization 2000, 2000.
- [21] K. DECKELNICK, G. DZIUK, AND C. M. ELLIOTT, *Computation of geometric partial differential equations and mean curvature flow*, Acta Numer., 14 (2005), pp. 139–232.
- [22] P. DU, M. KHENNER, AND H. WONG, *A tangent-plane marker-particle method for the computation of three-dimensional solid surfaces evolving by surface diffusion on a substrate*, J. Comput. Phys., 229 (2010), pp. 813–827.
- [23] I. FONSECA, A. PRATELLI, AND B. ZWICKNAGL, *Shapes of epitaxially grown quantum dots*, Arch. Ration. Mech. Anal., 214 (2014), pp. 359–401.
- [24] Y. GIGA, *Surface evolution equations*, Springer, 2006.
- [25] M. E. GURTIN AND M. E. JABBOUR, *Interface evolution in three dimensions with curvature-dependent energy and surface diffusion: Interface-controlled evolution, phase transitions, epitaxial growth of elastic films*, Archive for rational mechanics and analysis, 163 (2002), pp. 171–208.
- [26] K. HAUFFE, *The application of the theory of semiconductors to problems of heterogeneous catalysis*, in Advances in Catalysis, vol. 7, Elsevier, 1955, pp. 213–257.
- [27] F. HAUSSEER AND A. VOIGT, *A discrete scheme for parametric anisotropic surface diffusion*, J. Sci. Comput., 30 (2007), pp. 223–235.
- [28] D. W. HOFFMAN AND J. W. CAHN, *A vector thermodynamics for anisotropic surfaces: I. fundamentals and application to plane surface junctions*, Surface Science, 31 (1972), pp. 368–388.
- [29] W. JIANG, W. BAO, C. V. THOMPSON, AND D. J. SROLOVITZ, *Phase field approach for simulating solid-state dewetting problems*, Acta Mater., 60 (2012), pp. 5578–5592.
- [30] W. JIANG, Y. WANG, Q. ZHAO, D. J. SROLOVITZ, AND W. BAO, *Solid-state dewetting and island morphologies in strongly anisotropic materials*, Scr. Mater., 115 (2016), pp. 123–127.
- [31] W. JIANG AND Q. ZHAO, *Sharp-interface approach for simulating solid-state dewetting in two dimensions: A Cahn–Hoffman ξ -vector formulation*, Phys. D, 390 (2019), pp. 69–83.
- [32] Y. LI AND W. BAO, *An energy-stable parametric finite element method for anisotropic surface diffusion*, J. Comput. Phys., 446 (2021), p. 110658.
- [33] Z. LI, H. ZHAO, AND H. GAO, *A numerical study of electro-migration voiding by evolving level set functions on a fixed cartesian grid*, J. Comput. Phys., 152 (1999), pp. 281–304.

- [34] W. W. MULLINS, *Theory of thermal grooving*, J. Appl. Phys., 28 (1957), pp. 333–339.
- [35] M. NAFFOUTI, R. BACKOFEN, M. SALVALAGLIO, T. BOTTEIN, M. LODARI, A. VOIGT, T. DAVID, A. BENKOUIDER, I. FRAJ, L. FAVRE, ET AL., *Complex dewetting scenarios of ultrathin silicon films for large-scale nanoarchitectures*, Sci. Advances, 3 (2017), p. 1472.
- [36] P. SIMULATION, *Cfdtool - matlab cfd simulation gui & toolbox*, github. <https://github.com/precise-simulation/cfdtool/releases/tag/1.8.3>, 2022.
- [37] J. E. TAYLOR, *Mean curvature and weighted mean curvature*, Acta Metall. Mater., 40 (1992), pp. 1475–1485.
- [38] J. E. TAYLOR AND J. W. CAHN, *Linking anisotropic sharp and diffuse surface motion laws via gradient flows*, J. Stat. Phys., 77 (1994), pp. 183–197.
- [39] J. E. TAYLOR, J. W. CAHN, AND C. A. HANDWERKER, *Overview no. 98 i—geometric models of crystal growth*, Acta Metallurgica et Materialia, 40 (1992), pp. 1443–1474.
- [40] C. V. THOMPSON, *Solid-state dewetting of thin films*, Annu. Rev. Mater. Res., 42 (2012), pp. 399–434.
- [41] Y. WANG, W. JIANG, W. BAO, AND D. J. SROLOVITZ, *Sharp interface model for solid-state dewetting problems with weakly anisotropic surface energies*, Phys. Rev. B, 91 (2015), p. 045303.
- [42] A. WHEELER, *Cahn–Hoffman ξ -vector and its relation to diffuse interface models of phase transitions*, J. Stat. Phys., 95 (1999), pp. 1245–1280.
- [43] L. XIA, A. F. BOWER, Z. SUO, AND C. SHIH, *A finite element analysis of the motion and evolution of voids due to strain and electromigration induced surface diffusion*, J. Mech. Phys. Solids, 45 (1997), pp. 1473–1493.
- [44] Y. XU AND C.-W. SHU, *Local discontinuous Galerkin method for surface diffusion and Willmore flow of graphs*, J. Sci. Comput., 40 (2009), pp. 375–390.
- [45] J. YE AND C. V. THOMPSON, *Mechanisms of complex morphological evolution during solid-state dewetting of single-crystal nickel thin films*, Appl. Phys. Lett., 97 (2010), p. 071904.
- [46] Q. ZHAO, W. JIANG, AND W. BAO, *A parametric finite element method for solid-state dewetting problems in three dimensions*, SIAM J. Sci. Comput., 42 (2020), pp. B327–B352.